Journal of Molecular Spectroscopy **200,** 104–119 (2000)
doi:10.1006/jmsp.1999.8039, available online at http://www.idealibrary.com on IDEAL®

Characterization of the Ground State of Br_2 by Laser-Induced Fluorescence Fourier Transform Spectroscopy of the $B^3\Pi_{0^+u}$–$X^1\Sigma_g^+$ System

C. Focsa,[1] H. Li, and P. F. Bernath

Department of Chemistry, University of Waterloo, Waterloo, Ontario, Canada N2L 3G1

Received September 16, 1999; in revised form November 30, 1999

The laser-induced fluorescence (LIF) spectrum of the $B^3\Pi_{0^+u}$–$X^1\Sigma_g^+$ system of Br_2 was recorded by Fourier transform spectroscopy (FTS). The LIF spectra were obtained by using continuous-wave dye laser excitation in the spectral region 16 800–18 000 cm^{-1}. About 1800 rotationally resolved lines were recorded in 96 fluorescence progressions, originating from the $10 \le v' \le 22$ vibrational levels of the $B^3\Pi_{0^+u}$ state and involving the $2 \le v'' \le 29$ levels of the $X^1\Sigma_g^+$ ground state of the three isotopomers of bromine, $^{79}Br_2$, $^{81}Br_2$, and $^{79,81}Br_2$. These data, together with $^{79}Br_2$ data from a previous FTS absorption study [S. Gerstenkorn, P. Luc, A. Raynal, and J. Sinzelle, *J. Phys. (France)* **48,** 1685–1696 (1987)], were analyzed to yield improved Dunham constants for the ground state. A Rydberg–Klein–Rees (RKR) potential energy curve was computed for the $X^1\Sigma_g^+$ state ($v'' = 0$–29). The equilibrium bond length was found to be $R_e(X^1\Sigma_g^+) = 2.2810213(20)$ Å.

I. INTRODUCTION

The diatomic halogens and interhalogens have been the subject of numerous spectroscopic and kinetic studies. One of the main potential applications of halogens is as visible laser sources. In this context, molecular bromine has received considerable attention and is one of the halogens that has lased. The absorption spectrum of bromine in the visible region (to the red of 5100 Å) consists of two band systems, a more intense one ($B^3\Pi_{0^+u}$–$X^1\Sigma_g^+$) and a weaker one ($A^3\Pi_{1u}$–$X^1\Sigma_g^+$). The spectroscopy of the $B^3\Pi_{0^+u}$–$X^1\Sigma_g^+$ system is well documented, and we will give a detailed history of the spectroscopic studies concerning this system. There are also considerable data available on the radiative and collisional dynamics of the $B^3\Pi_{0^+u}$ state (e.g., Refs. (*1–5*); see also Ref. (*6*) for a very good review). Lasing of the $B^3\Pi_{0^+u}$–$X^1\Sigma_g^+$ system was demonstrated by Wodarczyk and Schlossberg (*7*) using a frequency-doubled Nd:YAG laser as a pump.

Since the first tentative vibrational analysis by Kuhn in 1926 (*8*) of the bromine visible bands, numerous studies have been devoted to the improvement of the spectroscopic knowledge. The first consistent analysis of the main absorption system of Br_2 was given by Brown in the early 1930s (*9, 10*). He performed first the vibrational analysis (*9*) of the bandheads involving the $0 \le v'' \le 5$ and $4 \le v' \le 48$ vibrational levels, correcting the previous assignment by Kuhn (*8*). Then he rotationally analyzed (*10*) a group of bands (with $2 \le v'' \le 4$ and $7 \le v' \le 13$) of the main $^{79,81}Br_2$ isotopomer. About the same time, Mulliken (*11–13*) established the $^3\Pi_{0^+u}$–$X^1\Sigma_g^+$ electronic assignment for the main visible system of Br_2.

After these early studies, the spectroscopy of the visible spectrum of the molecular bromine seems to have lanquished for about 30 years. The one exception was the vibrationally resolved work of Darbyshire in 1937 on $^{79,81}Br_2$ (*14*). He focused mainly on the "extreme red" $A^3\Pi_{1u}$–$X^1\Sigma_g^+$ system, but also recorded the near-infrared bands of the main $B^3\Pi_{0^+u}$–$X^1\Sigma_g^+$ system, involving the $4 \le v'' \le 14$ and $0 \le v' \le 12$ vibrational levels. In the 1960s interest in the absorption spectrum of Br_2 was renewed, with the 1967 work of Horsley and Barrow (*15*). They recorded separately the $^{79}Br_2$ and $^{81}Br_2$ $B^3\Pi_{0^+u}$–$X^1\Sigma_g^+$ spectra in the 5100–6200 Å region and rotationally analyzed bands involving the $0 \le v'' \le 3$ and $9 \le v' \le 19$ vibrational levels. They also studied several v'–0 bands involving v' levels immediately below the dissociation limit. About the same time, Clyne and Coxon (*16*) recorded a vibrationally resolved emission spectrum of Br_2 formed by atomic recombination.

In 1971, Coxon (*17*) recorded at high resolution the $B^3\Pi_{0^+u}$–$X^1\Sigma_g^+$ absorption system of $^{79}Br_2$ in the range 6350–7700 Å. He derived a set of accurate rovibrational constants for this isotopomer from the analysis of 28 new bands with $1 \le v' \le 9$ and $4 \le v'' \le 10$. He subsequently used his experimental data to calculate RKR potential energy curves for the $X^1\Sigma_g^+$ and $B^3\Pi_{0^+u}$ states (*18*), as well as Franck–Condon factors and *r*-centroids for the $B^3\Pi_{0^+u}$–$X^1\Sigma_g^+$ system (*19*). In 1974, Barrow *et al.* (*20*) published a quite complete (including rotational analysis, Franck–Condon factors, and long-range potential in the $B^3\Pi_{0^+u}$ state) study of the *B–X* system from separate observations of the absorption spectra of $^{79}Br_2$ and $^{81}Br_2$. The

[1] Present address: Laboratoire de Physique des Lasers, Atomes et Molécules, UMR CNRS, Centre d'Etudes et de Recherches Lasers et Applications, Université des Sciences et Technologies de Lille, 59 655 Villeneuve d'Ascq Cedex, France.

0022-2852/00 $35.00

vibrational levels involved were $0 \leq v'' \leq 10$ and $0 \leq v' \leq 55$ for the $^{79}Br_2$ isotopomer and $0 \leq v'' \leq 3$ and $v' = 9$, 11–13, 16, 19, and 39–54 for the $^{81}Br_2$ one.

The work of Barrow *et al.* (*20*) remained the reference study until the mid-eighties when Gerstenkorn *et al.* recorded a very good Fourier transform absorption spectrum of $^{79}Br_2$ in the region 11 600–19 600 cm^{-1}, which they published in the form of an atlas (*21*). Gerstenkorn *et al.* (*22*) later undertook an extensive analysis of these data, obtaining very good molecular constants for the $B^3\Pi_{0^+u}$–$X^1\Sigma_g^+$ system (with $0 \leq v'' \leq 14$ and $0 \leq v' \leq 52$). Gerstenkorn and Luc (*23*) also used these data to study the long-range potential of $^{79}Br_2$ in the $B^3\Pi_{0^+u}$ state. The Br_2 work of Gerstenkorn, Luc, and their co-workers is not well-known by the spectroscopic community because, for example, Franklin *et al.* (*24*) recorded a second Fourier transform absorption spectrum of the $^{79}Br_2$ $B^3\Pi_{0^+u}$–$X^1\Sigma_g^+$ system and performed an analysis of bands including $0 \leq v'' \leq 5$ and $6 \leq v' \leq 39$. In our opinion, however, the analysis of Gerstenkorn *et al.* (*22*) provides the most reliable high-resolution data for the $B^3\Pi_{0^+u}$–$X^1\Sigma_g^+$ system of Br_2 and their constants will be used extensively in the present work. Our work will focus on the $X^1\Sigma_g^+$ ground state and spectroscopic information concerning this state could also be derived from the $A^3\Pi_{1u}$–$X^1\Sigma_g^+$ extreme red system (*9, 14, 16, 25–28*). However, the $X^1\Sigma_g^+$ information derived from the study of the *A*–*X* system was always less extensive than that derived from the study of the "main" *B*–*X* system.

Since the early works of the 1930s, the very complex appearance of the visible absorption spectrum of bromine has been remarked. This complexity is due to the fact that natural bromine contains two isotopic species, ^{79}Br and ^{81}Br, of nearly equal abundance (50.69 and 49.31%, respectively (*29*)). Consequently, the rotational analysis of the visible spectrum of natural bromine turns out to be very difficult (in spite of the intrinsically simple *P*–*R* structure of the $^3\Pi_{0^+u}$–$X^1\Sigma_g^+$ transition), because three closely overlapping isotopic bands are present, due to $^{79}Br_2$, $^{79,81}Br_2$, and $^{81}Br_2$ (with a 1:2:1 intensity ratio). Accordingly, most studies were carried out using samples of isotopically pure $^{79}Br_2$ or $^{81}Br_2$.

Another effective method to overcome the spectral congestion would be to use the selective resonance fluorescence technique. Several authors have already used this technique for the study of the $X^1\Sigma_g^+$ ground state of Br_2. In 1964, Rao and Venkateswarlu (*30*) used a bromine atomic line to excite molecular bromine in the vacuum ultraviolet region. They recorded a *P*–*R* doublet series from 1565–1865 Å involving the $X^1\Sigma_g^+$ ground state of $^{79,81}Br_2$ up to $v'' = 36$. Their data were used by Le Roy and Burns (*31*) to obtain an RKR potential curve for the ground state up to $v'' = 36$. However, the rotational assignment of Rao and Venkateswarlu (*30*) was erroneous, as noticed by Coxon (*17*) from a comparison with his improved rotational constants. This assignment was changed by Venkateswarlu *et al.* (*32*) in 1982, when they used four atomic bromine lines to record 12 fluorescence series, involving the $v'' = 0$–76 vibrational levels of $^{79,81}Br_2$. Finally, in 1997, Franklin *et al.* (*24*), in addition to their absorption measurements, used a pulsed dye laser to excite the fluorescence of the $B^3\Pi_{0^+u}$–$X^1\Sigma_g^+$ system of $^{79,81}Br_2$. They measured 102 vibrational bands with $1 \leq v'' \leq 27$ and $15 \leq v' \leq 21$ but did not resolve any rotational structure. A more detailed discussion of the last two studies will be given in Section IV. Some other workers have studied the laser-induced fluorescence of the *B*–*X* system of Br_2, using either an argon ion laser (*33–36*) or a krypton ion laser (*37, 38*). However, they did not perform a spectroscopic analysis and limited their studies to the identification of the rovibrational levels involved.

We report here a laser-induced fluorescence study on the $B^3\Pi_{0^+u}$–$X^1\Sigma_g^+$ system of Br_2. Using a cw dye laser to excite the fluorescence of the natural bromine and a Fourier transform spectrometer to record it, we were able to observe about 1800 rotational lines in 96 fluorescence progressions, involving the $2 \leq v'' \leq 29$ and $10 \leq v' \leq 22$ vibrational levels. An extended characterization of the $X^1\Sigma_g^+$ ground state of the three Br_2 isotopomers was achieved up to $v'' = 29$.

II. EXPERIMENTAL DETAILS

A Coherent 599-01 cw linear dye laser, pumped by 6 W visible radiation from a Coherent Innova 70 argon ion laser, was used to excite the fluorescence of the $B^3\Pi_{0^+u}$–$X^1\Sigma_g^+$ system of Br_2. We used Rhodamine 6G and Rhodamine 110 dyes to cover the 16 800–18 000 cm^{-1} spectral region. The bandwidth of the dye laser was narrowed (triple-mode operation, FWHM $\cong$ 0.18 cm^{-1}) by placing a thin étalon inside the cavity, in order to excite a smaller number of transitions in the very dense *B*–*X* spectrum of Br_2. The dye laser power was typically in the range 0.5–1 W, depending on the spectral region.

The laser beam was focused in the center of a 15-cm long, 3-cm diameter glass cell containing the Br_2 vapor. We did not use isotopically pure Br_2, i.e., we had the three Br_2 isotopomers $^{79}Br_2$, $^{79,81}Br_2$, and $^{81}Br_2$ with their natural abundance in the cell. The bottom part of the cell was dry-ice cooled (at about -55°C) to obtain a Br_2 vapor pressure of about 1 Torr in order to prevent the quenching of the fluorescence by collisions. Attempts to record the Br_2 fluorescence with the cell at room temperature were unsuccessful. We performed a preliminary visual search for strong fluorescence signals by adjusting the birefringent filter of the dye laser. A total of 36 favorable laser line positions were selected in this way in the 16 800–18 000 cm^{-1} spectral region. At each of these laser positions several (usually between two and four) molecular transitions were excited, due to the very high degree of congestion of the *B*–*X* spectrum of Br_2 in this region.

Once a laser line was selected, the Br_2 cell was placed in front of a Bruker IFS 120 HR Fourier transform spectrometer (modified to record double-sided interferograms), and the central region of the cell was focused on the entrance aperture. We used either a photomultiplier tube or a Si photodiode to record

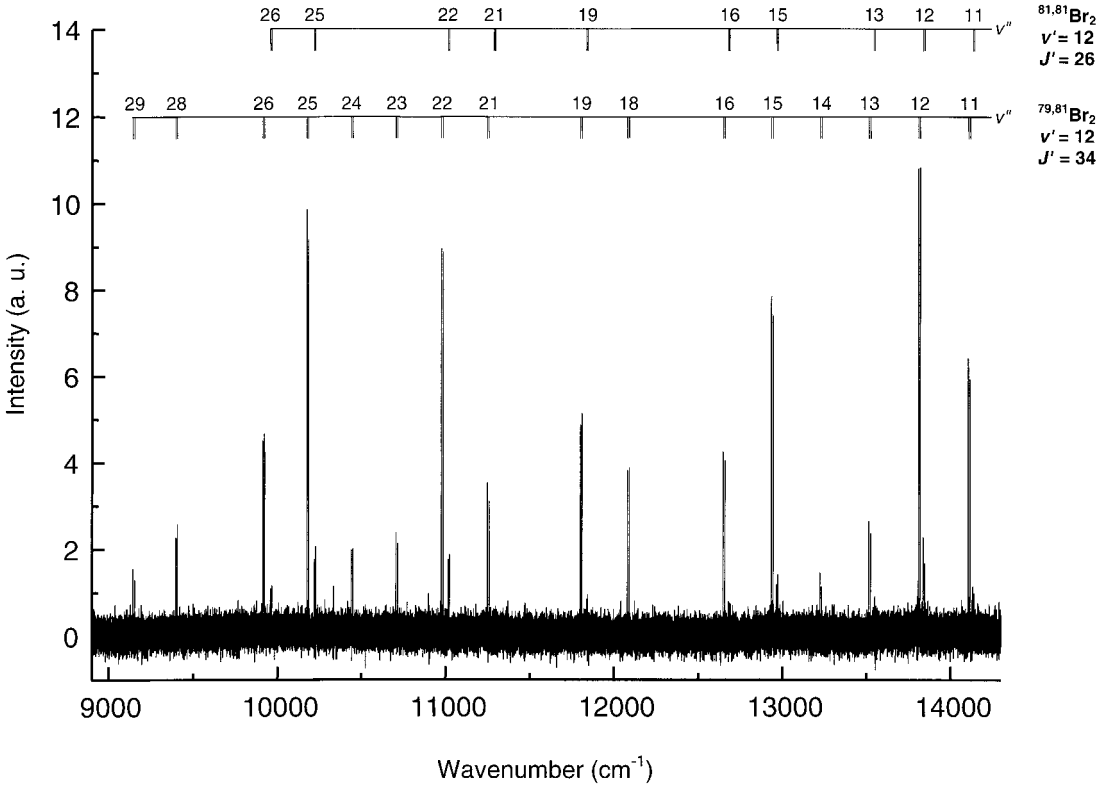

FIG. 1. Two *P–R* doublet fluorescence progressions, belonging to $^{79,81}Br_2$ (originating from the $v' = 12$, $J' = 34$ rovibrational level) and $^{81}Br_2$ $v' = 12$, $J' = 26$) simultaneously excited by a laser line placed at 16 883.908 cm^{-1}. The experimentally observed v'' vibrational levels of the $X^1\Sigma_g^+$ ground state are also indicated.

the 10 532–21 000 and the 8000–15 798 cm^{-1} spectral regions, respectively, at an instrumental resolution of 0.1 cm^{-1}. We also tried to record the fluorescence spectrum of the $B^3\Pi_{0^+u}$–$X^1\Sigma_g^+$ system of Br_2 in the near infrared (at wavenumbers <9000 cm^{-1}) using an InSb detector, but our attempts were unsuccessful. The use of a Ge photodiode detector in this region would be more effective, but such a detector was not available to us. We must emphasize that the Br_2 fluorescence is very weak (for example, compared to the I_2 fluorescence (*39*)) and we had to coadd 100 scans in about 3 h of observation in order to get a good signal-to-noise ratio.

The line positions were measured by fitting Voigt lineshape functions to the experimental lines in a nonlinear, least-squares procedure. The precision of our measurements is estimated to be about ± 0.005 cm^{-1} for strong, unblended lines. The air-to-vacuum conversion of the wavenumbers was done using Edén's formula (*40, 41*). Some details about the calibration of the spectra and the absolute accuracy of our line positions will be given in the next section.

III. ANALYSIS

1. Assignment of the Fluorescence Progressions

The fluorescence spectrum of the $B^3\Pi_{0^+u}$–$X^1\Sigma_g^+$ system of Br_2 consists of progressions of *P–R* doublets, originating from a common (v', J') rovibrational level of the $B^3\Pi_{0^+u}$ upper state and ending on different v'' (v'', $J'' = J' - 1$) and (v'', $J'' = J' + 1$) (for *R* and *P* lines, respectively) levels of the $X^1\Sigma_g^+$ lower state. An illustration of such a spectrum is given in Fig. 1, which displays two progressions, belonging to two different isotopomers ($^{79,81}Br_2$ and $^{81}Br_2$) and originating from the ($v' = 12$, $J' = 34$) and ($v' = 12$, $J' = 26$) upper levels, respectively, which are simultaneously excited by the laser line placed at 16 883.908 cm^{-1}. As one can easily see in Fig. 1, the *P–R* doublets corresponding to some v'' doublets are missing, in agreement with the Franck–Condon factors for the (v', v'') bands of the $B^3\Pi_{0^+u}$–$X^1\Sigma_g^+$ system (*19, 22*). It should be noted that the Br_2 fluorescence spectra were strictly resonant, i.e., no rotational or vibrational relaxation has been observed in the upper state.

To have a closer look at the *P–R* doublets corresponding to a given v'' vibrational level of the $X^1\Sigma_g^+$ lower state, Fig. 2 displays an interesting situation where no less than six (v', J') rovibrational levels of the $B^3\Pi_{0^+u}$ upper state were simultaneously excited by the laser line situated at 17 078.171 cm^{-1}. Notice that all three isotopomers of Br_2 are present in the spectrum displayed in Fig. 2, each of them with two *P–R* doublets. Although the assignment of spectra such as the one presented in Fig. 2 might seem difficult, it was quite straightforward, as can be seen from the description given below.

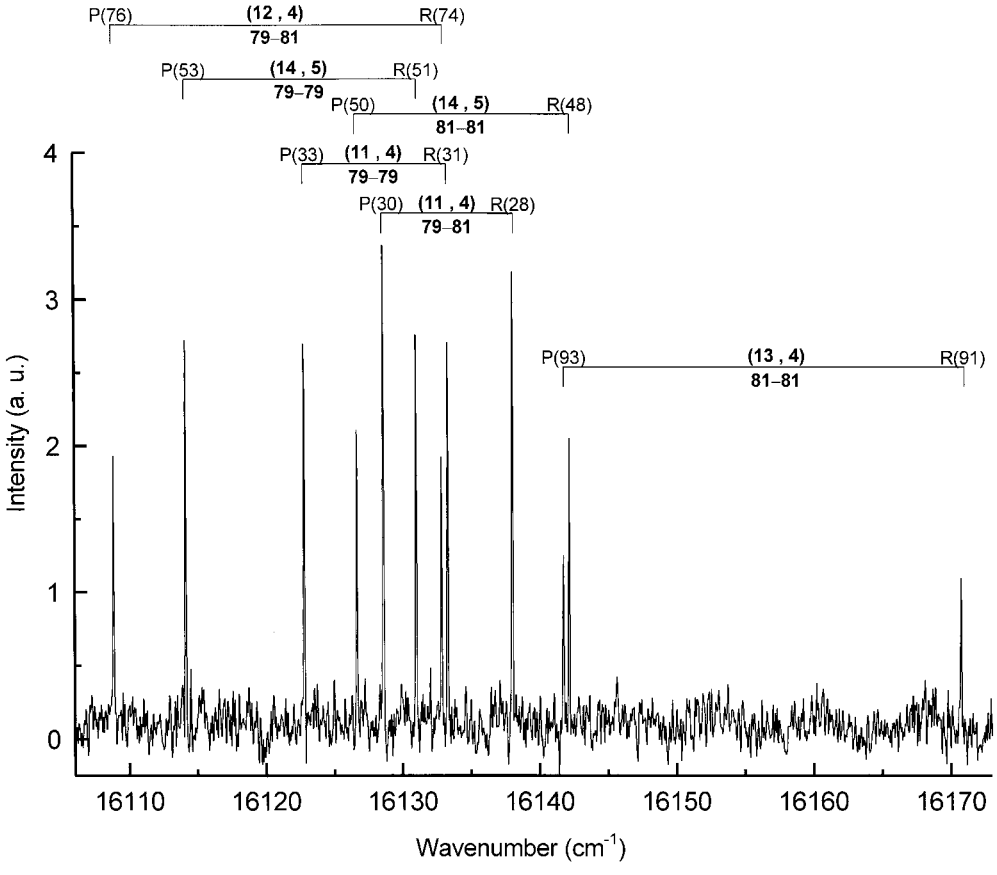

FIG. 2. An expanded portion of a fluorescence spectrum of the $B^3\Pi_{0^+u}$–$X^1\Sigma_g^+$ system of Br_2. The P–R doublets corresponding to the six (v', J') rovibrational levels of the $B^3\Pi_{0^+u}$ upper state (simultaneously excited by the laser line situated at 17 078.171 cm^{-1}) are displayed. For each doublet, the isotopomer, the (v', v'') vibrational assignment, as well as the P ($J'' = J' + 1$)–R ($J'' = J' - 1$) rotational assignment, are indicated.

In the assignment of the fluorescence series, we started with a visual inspection of the spectra, looking for clearly defined progressions such as the ones displayed in Fig. 1. Once such a progression was identified, the next step was to assign it with v and J quantum numbers. One can obtain a rough estimate of the J' quantum number by taking into account the fact that, neglecting centrifugal distortion, the separation between the $P(J' + 1)$ and the $R(J' - 1)$ lines belonging to a P–R doublet for a given v'' is expressed by the approximate relation:

$$\Delta\nu_{P-R} = \nu_{R(J'-1)} - \nu_{P(J'+1)} = \Delta_2 F''_{v''}(J') \cong 4B_{v''}(J' + \tfrac{1}{2}). \quad [1]$$

At this stage of the work we can use a typical value for $B_{v''}$ (say 0.08 cm^{-1}) regardless of the actual v'' and of the isotopomer involved in the progression, as our goal is to get only a rough estimate of J'. In addition, a guess of the v'' number can be obtained from the difference between the position of the P–R doublet considered and the position of the laser line. The vibrational constant for the $X^1\Sigma_g^+$ lower state is about 325 cm^{-1}, and the laser excites only molecules found in the first several vibrational levels of the ground state (usually $v \leq 3$), due to the relatively low temperature of the cell.

With these preliminary estimates of v'' and J' (or, equivalently, J'') quantum numbers, we proceeded to assign our fluorescence series by using the DSParFit program developed by Professor R. J. Le Roy at the University of Waterloo (illustrative applications of this program can be found in Refs. (*42–48*)). At this stage of the work, the very good rovibrational constants derived by Gerstenkorn *et al.* (*22*) from their absorption study of the $B^3\Pi_{0^+u}$–$X^1\Sigma_g^+$ system of Br_2 were of great help. The DSParFit program is able (among other features) to fit directly the fluorescence series while varying only the lower state spectroscopic constants and the energies of the various excited state levels. The energy of the upper (v', J') rovibrational level (common to all the transitions belonging to a given fluorescence progression) is varied in the fit, but is represented as just an energy value E, without concern about the particular quantum numbers associated with it. The Gerstenkorn *et al.* (*22*) Dunham constants accounting for the $v'' = 0$–14 $X^1\Sigma_g^+$ state of $^{79}Br_2$ were introduced into (and held fixed by) the program. The corresponding constants for the two other isotopomers were automatically calculated by the program using the

customary dependence on the reduced masses, assuming that the Born–Oppenheimer and first-order semiclassical approximations are valid. Several trial assignments were automatically generated for the progression around the (v'', J') values estimated in the manner described above, for all three isotopomers of Br_2. In this way one set of data was tested by several tens of "trial" sets of (v'', J', isotopomer) numbers, but after running the program only one of these assignments (the correct one) was consistent with the $X^1\Sigma_g^+$ constants. Of course this agreement was better for $v'' \leq 14$ and slowly deteriorated as we went higher in v'', but the correct assignment still had a much smaller standard deviation than the other trial ones. In addition to this procedure, we alternatively used a PC program developed by one of us (H.L.) to aid in the assignments. This program used the constants of both upper and lower states (*22*) in order to find a match between the experimental line positions and the calculated ones. The results obtained by the two programs were the same, giving us a positive test for the validity of our assignments.

In this way we were able to assign 96 fluorescence progressions involving all three isotopomers of Br_2. Several of these progressions were excited twice (by very close positions of the laser line), so only 85 of them are distinct. A listing of these 85 fluorescence excitation transitions is given in Table 1, together with the range ($v''_{\min}$, $v''_{\max}$) of the ground state vibrational levels observed, the assignment (v', J') $\leftarrow$ (v'', J'') of the line excited by the laser and its position calculated from the Gerstenkorn *et al.* (*22*) constants. The Gerstenkorn *et al.* (*22*) constants describe very well the $v'' = 0$–14 and the $v' = 0$–48 regions of the potential curves of the $X^1\Sigma_g^+$ and $B^3\Pi_{0^+u}$ states, respectively, and, as one can see from Table 1, our excitation lines involved only the vibrational levels $v'' = 0$–3 and $v' = 10$–22.

Several remarks can be made about the information listed in Table 1. First of all, the range $v'' = 0$–14 covered by the high-resolution absorption study of Gerstenkorn *et al.* (*22*) has now been extended to $v''_{\max} = 29$. We have two kinds of fluorescence progressions: the "long" ones, with $v''_{\max}$ up to 29, and the "short" ones, with $v''_{\max}$ up to 14, corresponding to the spectra recorded with the Si photodiode (which extended down to $\sim$9000 cm^{-1}) or the photomultiplier tube (which extended only to $\sim$13 500 cm^{-1}), respectively. The range of rotational levels covered by our measurements ($J'' = 4$–109) is comparable to that of Gerstenkorn *et al.* (*22*). As the Br_2 molecules were at relatively low temperature, it might seem curious that among the 85 excitation lines listed in Table 1, only three of them have $v'' = 0$ as lower state, while most of them originate from the $v'' = 2$ vibrational level. As already noted by Coxon (*19*) and Gerstenkorn *et al.* (*22*), the $q_{v',0}$ Franck–Condon factors have very small values, with a maximum around $v' = 30$ (and this spectral region, at wavenumbers higher than 19 000 cm^{-1}, was not accessible with our laser).

Our experimental data are simultaneously obtained for all three isotopomers of Br_2, while the previous studies have generally used one isotopomer at a time (for instance, $^{79}Br_2$ in the case of Gerstenkorn *et al.* (*21–23*) or Coxon (*17*), or $^{79}Br_2$ and $^{81}Br_2$ (separately) in the case of Barrow *et al.* (*20*)) in order to reduce the congestion of the absorption spectrum. This situation gives us the opportunity to test the validity of the Born–Oppenheimer and semiclassical quantum number scaling approximations for Br_2 on a consistent set of data recorded simultaneously. Note, however, that the major part of the data summarized in Table 1 belong to the $^{79,81}Br_2$ isotopomer: 1182 rotational lines in 59 fluorescence progressions, compared to 257 lines in 16 progressions for $^{79}Br_2$ and 345 lines in 21 progressions for $^{81}Br_2$.

Once the assignment of the fluorescence lines was completed, we could proceed to the absolute calibration of the wavenumber scale. In the absence of atomic lines, we decided to calibrate our spectra against Br_2 line positions calculated using the constants of Gerstenkorn *et al.* (*22*). We used lines of the three isotopomers in the range 13 000–17 000 cm^{-1}, involving the vibrational levels $v'' = 2$–14 and $v' = 10$–22, for which the constants of Gerstenkorn *et al.* (*22*) are very reliable and reproduce our data very well. Unfortunately we did not have the list of Gerstenkorn *et al.*'s assignments, but we still could compare the result of our calibration with the lines given in their atlas (without the assignments) for the $^{79}Br_2$ isotopomer. Several tens of common lines were identified for this isotopomer, and the difference between our calibrated wavenumbers and theirs (Gerstenkorn *et al.* (*21, 22*) calibrated their $^{79}Br_2$ data against the molecular lines of iodine) was less than 0.01 cm^{-1}, which provides a good estimate of our absolute accuracy.

2. *Least-Squares Treatment: Determination of the Dunham Parameters*

The experimental lines were fitted in an iterative, least-squares procedure using the DSParFit program mentioned above. Each datum was weighted with the square of the reciprocal of the estimated uncertainty. The major part of the lines were assigned a weighting factor of 0.01 cm^{-1}, while some of them (the weaker ones) were deweighted to 0.03 or 0.05 cm^{-1}. To improve the fit, the $^{79}Br_2$ ground state term values for the $v'' = 0$–14, $J'' = 0$–100 were calculated using the constants of Gerstenkorn *et al.* (*22*) and introduced in our set of data as a fluorescence series originating from a "virtual" energy level situated at 20 000 cm^{-1} (one can choose any other value, of course). These data were weighted at 0.002 cm^{-1}, in agreement with the precision estimated by Gerstenkorn *et al.* (*22*). This procedure has the effect of constraining our derived spectroscopic constants to reproduce the results of Gerstenkorn *et al.* (*22*), but the resulting statistics need to be interpreted with care. The final data set was made up of a total of 3299 data: 1784 experimental lines in 96 fluorescence progressions belonging to the three isotopomers, and 1515 synthetic term values for the ground state of the $^{79}Br_2$ isotopomer.

TABLE 1
Summary of the 85 Distinct Fluorescence Progressions of the $B^3\Pi_{0^+u}$–$X^1\Sigma_g^+$ System of Br_2 Observed in the Present Work

ν (cm^{-1})	Isotope	v'	v''	J''	v''_{min}	v''_{max}	ν (cm^{-1})	Isotope	v'	v''	J''	v''_{min}	v''_{max}
16810.3035	79 - 81	15	3	P(64)	10	29	17024.3344	79 - 81	11	1	P(52)	8	27
16810.3454	79 - 81	14	3	R(28)	8	27	17024.3350	79 - 81	13	2	R(18)	8	28
16810.4726	79 - 81	12	2	R(61)	4	26	17032.2742	79 - 79	11	1	P(51)	3	13
16847.5172	79 - 81	12	2	R(49)	4	28	17032.3025	79 - 79	13	2	P(11)	4	14
16861.4595	79 - 81	12	2	P(40)	4	26	17032.3239	79 - 81	14	2	P(60)	4	14
16861.6456	79 - 81	15	3	R(53)	6	29	17032.3257	79 - 81	13	2	R(4)	4	12
16861.7123	79 - 81	13	2	P(74)	4	28	17032.3865	79 - 81	11	1	R(53)	3	13
16861.7455	79 - 79	12	2	R(45)	4	26	17047.0415	79 - 81	16	3	P(10)	10	28
16877.0095	79 - 81	12	2	P(33)	4	28	17047.0978	79 - 81	15	2	P(81)	7	29
16883.8578	81 - 81	12	2	P(27)	4	26	17047.1167	79 - 79	14	2	P(57)	8	27
16883.9293	79 - 81	12	2	R(33)	4	29	17047.1453	79 - 81	11	1	P(44)	8	26
16899.2020	79 - 81	12	2	R(23)	4	28	17054.7587	79 - 81	11	1	P(41)	3	12
16899.2574	81 - 81	12	2	R(19)	4	28	17054.8022	79 - 81	14	2	R(57)	4	14
16905.9340	79 - 79	12	2	R(21)	5	25	17078.0814	79 - 79	11	1	P(33)	4	9
16905.9488	79 - 81	12	2	P(13)	5	25	17078.1467	79 - 79	14	2	R(51)	5	14
16906.0289	79 - 81	11	1	P(82)	4	23	17078.2357	81 - 81	14	2	R(48)	5	11
16906.0751	81 - 81	13	2	R(66)	5	28	17078.2981	79 - 81	11	1	P(30)	4	9
16906.1145	79 - 81	15	3	P(33)	10	29	17100.3017	79 - 81	11	1	P(14)	4	9
16906.6507	79 - 81	15	3	R(36)	6	29	17100.4463	79 - 79	11	1	R(33)	4	9
16906.6515	79 - 81	10	1	R(53)	4	27	17100.4571	79 - 81	12	1	P(65)	4	9
16906.7612	79 - 81	16	3	P(66)	6	28	17129.8580	81 - 81	14	2	P(19)	5	11
16906.7950	79 - 81	12	2	P(12)	4	12	17129.8857	79 - 81	15	2	P(63)	5	11
16906.8078	81 - 81	12	2	R(8)	4	12	17129.8862	79 - 81	12	1	P(57)	4	11
16920.6791	81 - 81	13	2	R(62)	5	25	17129.9435	81 - 81	17	3	P(24)	6	13
16920.7041	79 - 81	10	1	P(44)	4	27	17129.9588	81 - 81	12	1	R(59)	4	11
16943.0864	79 - 81	13	2	P(53)	4	28	17129.9775	81 - 81	17	3	R(27)	6	13
16957.6546	79 - 81	10	1	R(30)	3	27	17130.0013	81 - 81	15	2	P(62)	5	11
16958.5813	79 - 81	13	2	P(48)	4	28	17130.0374	79 - 81	14	2	R(26)	5	11
16958.6195	79 - 79	14	2	R(81)	8	27	17143.0596	79 - 79	14	2	R(20)	8	27
16972.5946	79 - 81	13	2	P(43)	7	25	17143.1885	79 - 81	12	1	P(53)	8	25
16973.4060	79 - 81	16	3	P(48)	6	14	17246.4885	79 - 79	15	2	P(23)	10	29
16973.4837	81 - 81	10	1	R(8)	3	10	17246.5273	79 - 81	14	1	P(83)	8	28
16973.4965	79 - 81	10	1	R(17)	2	12	17246.5822	81 - 81	16	2	P(59)	9	29
16973.5239	81 - 81	15	2	R(97)	4	10	17882.7249	79 - 81	15	0	R(25)	3	20
16973.5452	81 - 81	13	2	P(41)	4	12	17882.7393	79 - 81	18	1	P(14)	4	21
16987.4601	79 - 81	13	2	P(37)	4	28	17898.0652	79 - 81	15	0	P(7)	3	10
16987.5013	81 - 81	13	2	P(35)	4	28	17905.4069	79 - 79	19	1	P(49)	4	12
16989.6241	81 - 81	13	2	P(33)	4	12	17905.4773	79 - 81	22	2	R(27)	5	11
16989.7313	79 - 81	13	2	P(36)	4	11	17912.5723	79 - 81	22	2	R(23)	5	11
17002.8600	81 - 81	13	2	P(27)	7	24	17912.6564	79 - 81	19	0	R(107)	3	10
17002.8810	79 - 81	17	3	P(67)	9	25	17912.6808	79 - 79	22	2	P(24)	5	11
17017.0154	79 - 81	11	1	R(58)	8	27	17912.6911	79 - 79	21	1	R(85)	4	11
17017.0706	79 - 79	13	2	P(24)	8	27							

The $X^1\Sigma_g^+$ ground state rovibrational energies were represented by the conventional double Dunham expansion (*49*),

$$E_X(v'', J'') = \sum_{k,m} Y''_{k,m}\left(v'' + \frac{1}{2}\right)^k [J''(J'' + 1)]^m, \qquad [2]$$

while each of the 85 $B^3\Pi_{0^+u}$ rovibrational levels involved in the fluorescence progressions was fitted as an independent energy value. The DSParFit code deals with the Dunham constants for a selected reference isotopomer (which can be chosen by the user) and automatically includes the other isotopomers through their dependence on the reduced mass, op-

TABLE 2
Dunham Constants (in cm^{-1}) for the $X^1\Sigma_g^+$ Ground State of Br_2 (all uncertainties are 1σ)

k	$Y_{k,0}$	$Y_{k,1}$	$Y_{k,2}$
		$^{79}Br_2$	
0		$8.210886(15)\times10^{-2}$	$-2.0995(15)\times10^{-8}$
1	325.314194(320)	$-3.2057(5)\times10^{-4}$	$-8.1(4)\times10^{-11}$
2	-1.078688(100)	$-7.775(77)\times10^{-7}$	$-3.6(3)\times10^{-12}$
3	$-1.9942(150)\times10^{-3}$	$-7.8(5)\times10^{-9}$	
4	$-1.618(110)\times10^{-5}$	$-2.35(10)\times10^{-10}$	
5	$-1.1(4)\times10^{-7}$		
6	$-3.52(45)\times10^{-9}$		
		$^{79,81}Br_2$	
0		8.10951602×10^{-2}	-2.04798×10^{-8}
1	323.299825	-3.1465182×10^{-4}	-7.8523×10^{-11}
2	-1.065370731	-7.58421×10^{-7}	-3.4683×10^{-12}
3	-1.9573842×10^{-3}	-7.5615×10^{-9}	
4	-1.578296×10^{-5}	-2.26403×10^{-10}	
5	-1.066363×10^{-7}		
6	-3.39123×10^{-9}		
		$^{81}Br_2$	
0		8.00814605×10^{-2}	-1.9971×10^{-8}
1	321.2728263	-3.0877051×10^{-4}	-7.6092×10^{-11}
2	-1.052053462	-7.39579×10^{-7}	-3.3399×10^{-12}
3	-1.9207978×10^{-3}	-7.3274×10^{-9}	
4	-1.539084×10^{-5}	-2.18019×10^{-10}	
5	-1.03335×10^{-7}		
6	-3.26564×10^{-9}		

Note. The $^{79}Br_2$ values were directly returned by the combined isotopomer least-squares procedure, while the values corresponding to the two other isotopomers were calculated using their dependence on the reduced mass (see text).

tionally including terms to account for the breakdown of the Born–Oppenheimer approximation. In our case we chose $^{79}Br_2$ as the reference isotopomer. To the accuracy of the present data set, the simple first-order semiclassical mass scaling was found to be valid, so no atomic mass dependent correction terms were required.

To obtain a satisfactory fit, Dunham expansions of orders 6, 4, and 2 were needed for the G_v, B_v, and D_v parameters (i.e., $Y_{k,0}$, $Y_{k,1}$, and $Y_{k,2}$), respectively. The 3299 data were fitted to a total of 111 parameters: 14 Dunham constants, 96 energy values for the upper levels of the 96 fluorescence progressions, and one additional energy value, corresponding to the virtual upper level used to treat the calculated term values of the $X^1\Sigma_g^+$ ($v'' = 0$–14) ground state of $^{79}Br_2$ as a fluorescence series (see above).

The dimensionless standard deviation of the fit was of 0.41 and the Dunham constants obtained for the $X^1\Sigma_g^+$ ground state are listed in Table 2. The "sequential rounding and refitting" procedure of the DSParFit code (*43*) was used to minimize the number of digits that need to be reported in order to reproduce the experimental data. Only the $Y_{k,m}$ parameters for the $^{79}Br_2$ isotopomer (that we chose as reference isotopomer) were directly varied by the least-squares procedure, while the constants for the other two isotopomers were calculated through their dependence on the reduced mass

$$Y_{k,m} \propto \mu^{-(k+2m)/2} \qquad [3]$$

using $\mu(^{79}Br_2) = 39.4591689500$, $\mu(^{79,81}Br_2) = 39.9524135583$, and $\mu(^{81}Br_2) = 40.4581455000$, calculated from the isotopic masses given in Ref. (*29*), and as coded into a subroutine used by DSParFit. Note that the sequential rounding and fitting

TABLE 3

Observed Line Positions (in cm^{-1}) for the $B^3\Pi_{0^+u}$–$X^1\Sigma_g^+$ System of Br_2

$^{79}Br_2$

v''	R	P
	v'=14, J'=82,	E=18141.819(2)
8	15092.389(10)	15066.324(-3)
11	14189.992(0)	14164.258(-6)
12	13893.868(-18)	13868.264(-38)
14	13308.664(9)	13283.284(-5)
15	13019.667(11)	12994.401(0)
17	12448.989(-9)	12423.946(-5)
18	12167.321(3)	12142.405(0)
20	11611.521(1)	11586.854(-7)
21	11337.414(14)	11312.867(9)
23	10796.986(6)	10772.692(1)
24	10530.713(-1)	10506.525(16)
27	9748.022(-12)	9724.234(-3)
	v'=11, J'=50,	E=17571.747(2)
3	16410.563(8)	16394.231(5)
4	16094.789(0)	16078.520(0)
6	15469.928(-28)	15453.770(-6)
8	14854.009(-1)	14838.003(4)
9	14549.472(1)	14533.544(-2)
10		14231.379(-6)
12	13649.720(4)	13634.007(-7)
	v'=13, J'=23,	E=17709.968(2)
8	15146.307(-3)	15138.855(-5)
11	14237.630(-1)	14230.266(5)
12		13932.022(20)
14	13349.897(6)	13342.634(8)
17	12483.646(-4)	
21	11363.047(-1)	11356.023(1)
24	10549.301(-2)	10542.386(-1)
27		9752.519(-3)
	v'=15, J'=22,	E=17935.485(2)
10	14767.198(-4)	14760.121(-4)
11	14466.589(1)	14459.540(5)
13	13872.382(1)	13865.400(1)
14	13578.818(0)	13571.868(-2)
16	12998.860(0)	12991.967(5)
17	12712.504(7)	12705.655(0)
19	12147.193(-9)	12140.397(-3)
20	11868.249(6)	11861.494(4)
22	11317.996(-1)	11311.294(12)
23	11046.724(-4)	11040.071(-6)
25	10512.033(-7)	10505.441(-1)
26	10248.675(-5)	10242.126(-6)
28	9730.120(-5)	9723.639(-2)
29	9474.977(10)	9468.538(7)
	v'=11, J'=24,	E=17468.648(3)
4	16144.640(2)	16136.741(-1)
8	14901.338(-2)	14893.567(-2)
9	14596.156(5)	14588.426(-2)
	v'=12, J'=46,	E=17674.075(2)
4	16227.724(3)	16212.751(-7)
5	15914.033(7)	15899.117(0)
8	14986.447(-7)	14971.706(-2)
9	14681.782(-4)	14667.110(-5)
11	14079.360(-1)	14064.809(4)
12	13781.635(2)	13767.151(5)
15	12902.649(-1)	12888.356(5)
16	12614.428(16)	12600.223(0)
18	12045.355(-1)	12031.271(-3)
19	11764.509(6)	11750.497(0)
21	11210.376(-2)	11196.468(27)
22	10937.131(-5)	10923.315(0)
24	10398.424(-9)	10384.745(2)
25	10133.011(3)	10119.416(3)
26	9870.291(1)	9856.772(-2)
	v'=13, J'=10,	E=17687.153(2)
4	16400.396(4)	16397.014(1)
5	16086.059(2)	16082.689(-1)
7	15464.084(3)	15460.742(-1)
8	15156.481(0)	15153.150(0)
9	14851.151(0)	14847.839(-5)
10	14548.121(-8)	14544.809(0)
11	14247.379(4)	14244.094(0)
12	13948.982(-3)	13945.700(5)
14	13359.217(6)	13355.981(-3)
	v'=14, J'=56,	E=17959.793(2)
8	15192.159(-2)	15174.264(-2)
10	14585.820(-6)	14568.070(2)
11	14286.109(-2)	14268.447(-4)
12	13988.729(6)	
13	13693.721(-8)	13676.199(6)
14	13401.062(2)	13383.639(-4)
15	13110.799(8)	13093.451(7)
17	12537.555(-2)	12520.363(4)
18	12254.590(12)	12237.494(4)
20	11696.174(-3)	11679.235(-2)
21	11420.740(2)	11403.894(-5)
23	10877.599(-2)	10860.918(-3)
24	10609.939(-1)	10593.349(-5)
26	10082.606(2)	10066.193(-1)
27	9823.006(-2)	9806.681(-4)
	v'=22, J'=23,	E=18605.569(3)
5	16971.072(-4)	16963.523(-2)
6	16659.094(3)	16651.564(16)
8	16041.902(2)	16034.456(-5)
11	15133.231(-1)	15125.870(1)
	v'=12, J'=22,	E=17587.618(2)
5	15956.654(-3)	15949.421(3)
8	15027.437(6)	15020.309(-3)
11	14118.727(-4)	14111.683(-5)
12	13820.444(3)	13813.430(3)
15	12939.776(-6)	12932.847(2)
18	12080.741(3)	12073.917(3)
19	11799.318(0)	11792.537(-10)
21	11243.987(-4)	11237.260(-1)
22	10970.121(7)	10963.435(4)
24	10430.176(10)	10423.579(-14)
25	10164.155(3)	10157.577(-3)
	v'=11, J'=32,	E=17492.788(3)
4	16133.311(-1)	16122.834(-3)
8	14890.593(-3)	14880.277(6)
9	14585.567(-4)	14575.299(2)
	v'=14, J'=52,	E=17937.736(2)
5	16131.012(2)	16114.171(0)
6		15802.986(-5)
7	15510.743(-1)	15494.040(0)
8	15203.997(1)	15187.366(-2)
10	14597.364(-1)	14580.875(-2)
11	14297.511(-2)	14281.087(4)
14	13412.012(7)	13395.821(0)
	v'=14, J'=21,	E=17821.327(2)
8	15264.491(-9)	15257.674(-11)
10	14656.330(7)	14649.574(2)
11	14355.715(5)	14348.987(1)
14	13467.902(2)	13461.261(1)
17	12601.541(11)	12594.989(12)
20	11757.240(11)	
23	10935.672(-4)	10929.315(-7)
24	10666.993(-8)	10660.678(-20)
26	10137.569(1)	10131.313(-3)
27	9876.901(3)	9870.686(-8)
	v'=21, J'=86,	E=18831.397(4)
4	16963.523(-25)	
5	16651.564(-23)	16623.857(5)
6	16341.825(3)	16314.263(0)
9	15426.305(1)	15399.098(-6)
11		14800.477(18)
	v'=19, J'=48,	E=18428.415(3)
4		16951.451(6)
5		16637.891(4)
6	16342.063(3)	16326.566(2)
7		16017.490(0)
9	15421.448(-3)	15406.145(-3)
12		14506.398(-7)

Note. "Calculated − observed" differences are reported in parentheses, in the units of the last quoted digit. The lines are grouped in fluorescence progressions and labeled by the v' and J' quantum numbers of the upper rovibrational level. The $P(J'+1)$–$R(J'-1)$ lines are listed on the same row for each v'' ground state vibrational level observed. The term value E of each (v', J') upper rovibrational level is also displayed (with respect to the $X^1\Sigma_g^+$ ($v''=0$, $J''=0$) level for each isotopomer).

procedure applies only to the reference isotopomer and additional digits as indicated by the parameter sensitivity are required for the other two isotopomers (*42*, *43*).

The experimental lines, along with the "calculated − observed" differences (in parentheses) are listed in Table 3 (for reasons of space, only the lines belonging to the 85 distinct

TABLE 3—*Continued*

$^{79,81}Br_2$

v''	R	P
	$v'=12$, $J'=11$,	E=17559.499(2)
4	16279.029(0)	16275.366(-1)
5	15966.575(-1)	15962.926(-2)
7	15348.288(-4)	15344.665(-1)
8	15042.479(-1)	15038.871(3)
9	14738.918(0)	14735.329(0)
11	14138.597(5)	14135.051(-7)
12	13841.880(0)	13838.335(3)
	$v'=13$, $J'=47$,	E=17787.517(1)
4	16343.682(-6)	16328.566(-8)
5	16031.884(0)	16016.830(-3)
8	15109.804(-3)	15094.934(-3)
11	14207.981(-3)	14193.299(-1)
12	13911.950(-1)	13897.334(0)
14	13326.866(3)	13312.379(4)
15	13037.854(1)	13023.432(4)
17	12466.969(17)	12452.705(-6)
18	12185.169(4)	12170.956(-1)
19	11905.807(-1)	11891.660(-4)
20	11628.920(-12)	11614.825(2)
21	11354.504(2)	11340.494(0)
22	11082.622(4)	11068.682(2)
24	10546.546(-1)	10532.746(-1)
25	10282.404(-1)	10268.678(-1)
27	9762.077(0)	9748.501(-2)
28	9505.959(3)	9492.454(4)
	$v'=12$, $J'=24$,	E=17583.702(1)
4	16268.040(-13)	16260.230(-8)
5	15955.715(0)	15947.941(2)
8	15032.052(0)	15024.376(-1)
9	14728.644(-5)	14721.000(-6)
11	14128.620(-2)	14121.038(2)
12	13832.043(2)	13824.498(2)
13	13537.780(7)	13530.285(-9)
14		13238.398(-17)
15	12956.292(2)	12948.845(4)
16	12669.092(5)	12661.682(5)
18	12101.906(5)	12094.560(10)
19	11821.962(4)	11814.661(-1)
21	11269.493(3)	11262.257(4)
22	10997.024(-2)	10989.821(1)
23	10727.097(-7)	10719.918(9)
24	10459.723(8)	10452.616(-11)
25	10194.977(-2)	10187.887(0)
26	9932.851(2)	9925.807(-4)
28	9416.640(6)	9409.675(-1)
	$v'=11$, $J'=13$,	E=17438.394(3)
4	16154.260(0)	16149.958(1)
8	14917.763(6)	14913.542(-5)
9	14614.224(0)	14610.012(-1)
	$v'=12$, $J'=32$,	E=17607.260(2)
4	16256.553(-6)	16246.204(-7)
5	15944.380(-2)	15934.064(5)
8	15021.153(-7)	15010.963(2)
11	14118.154(-2)	14108.097(4)
12	13821.724(4)	13811.723(-2)
13	13527.587(33)	13517.637(20)
15	12946.426(3)	12936.558(-2)
16	12659.400(-13)	12649.562(-3)
18	12092.516(-5)	12082.768(7)
19	11812.705(19)	11803.030(5)
21	11260.583(-10)	11250.974(4)
22	10988.265(-4)	10978.710(4)
25	10186.717(-5)	10177.314(-1)
26	9924.755(5)	9915.402(9)
28	9408.904(-4)	9399.657(-5)
	$v'=15$, $J'=37$,	E=17970.182(1)
6	15970.494(-10)	15958.639(2)
8	15357.440(3)	15345.701(-3)
10	14753.399(-2)	14741.754(-2)
11	14454.793(-4)	14443.193(1)
13	13864.490(-3)	13852.998(-4)
14	13572.834(-2)	13561.389(1)
16	12996.604(2)	12985.260(9)
17	12712.076(3)	12700.790(5)
19	12150.306(1)	12139.124(5)
20	11873.113(-5)	11861.984(1)
22	11326.214(2)	11315.201(2)
23	11056.578(-2)	11045.621(-2)
25	10525.050(2)	10514.211(-2)
26	10263.233(-1)	10252.446(1)
28	9747.635(3)	9736.962(9)
29	9493.932(5)	9483.330(0)
	$v'=13$, $J'=73$,	E=17946.933(2)
4	16257.107(-13)	16233.743(-4)
5	15946.306(-2)	15923.045(0)
8	15027.265(-3)	15004.300(-7)
9	14725.420(-11)	14702.556(-19)
11	14128.540(0)	14105.867(-1)
12	13833.557(3)	13810.983(2)
14	13250.602(-1)	13228.234(-5)
15	12962.658(3)	12940.389(1)
17	12393.946(20)	12371.902(0)
18	12113.252(3)	12091.287(9)
19	11834.979(21)	11813.142(5)
21	11285.956(1)	11264.314(5)
22	11015.223(1)	10993.692(3)
24	10481.465(5)	10460.163(0)
25	10218.511(2)	10197.317(2)
27	9700.611(-12)	9679.630(4)
28	9445.713(2)	9424.869(-6)
	$v'=10$, $J'=54$,	E=17458.382(2)
4	15958.854(-3)	15941.512(-1)
8	14725.882(7)	14708.833(1)
9	14423.242(-1)	14406.262(-3)
10	14122.862(0)	14105.955(-3)
13	13235.504(1)	13218.813(4)
14	12944.383(-9)	12927.757(4)
16	12369.206(8)	12352.748(4)
17	12085.215(10)	12068.839(2)
20	11247.897(4)	11231.749(3)
21	10973.755(1)	10957.680(6)
23	10433.066(0)	10417.164(-5)
24	10166.580(-1)	10150.753(1)
25	9902.717(-12)	9886.960(3)
27	9382.919(5)	9367.363(-12)
	$v'=16$, $J'=65$,	E=18217.073(2)
6	15994.253(-1)	15973.598(-2)
8	15383.064(3)	15362.588(-4)
9	15080.849(0)	15060.450(4)
10	14780.903(1)	14760.598(-2)
11	14483.240(6)	14463.019(7)
13	13894.876(-10)	13874.826(-1)
16	13029.912(11)	13010.151(4)
17	12746.402(-9)	12726.717(0)
22	11365.646(11)	11346.456(2)
25	10567.686(15)	10548.808(-9)
26	10306.985(-11)	10288.174(0)
28	9793.608(1)	9775.021(-6)
	$v'=14$, $J'=29$,	E=17832.306(2)
8	15260.294(-4)	15251.052(-5)
10	14655.904(-5)	14646.735(0)
11	14357.117(-1)	14347.993(-1)
12	14060.614(17)	14051.548(-2)
13	13766.452(10)	13757.421(-3)
14	13474.630(-3)	13465.622(2)
15	13185.141(6)	13176.156(28)
17	12613.335(-4)	12604.451(0)
18	12331.046(-8)	12322.188(13)
20	11773.805(-4)	11765.051(-3)
21	11498.906(0)	11490.188(7)
23	10956.694(1)	10948.074(-4)
24	10689.430(2)	10680.857(-3)
26	10162.760(-7)	10154.268(-2)
27	9903.399(2)	9894.960(-1)
	$v'=13$, $J'=35$,	E=17736.835(3)
4	16370.358(0)	
5	16058.251(1)	16046.994(0)
7	15440.668(-2)	15429.502(-2)
8	15135.217(-2)	15124.097(-1)
11		14221.436(5)

fluorescence progressions summarized in Table 1 are displayed in Table 3). Although the v' and J' quantum numbers associated with the upper level of a fluorescence series are not important for the fitting program, they provide a practical label for the progressions and we accordingly used them in Table 3. Along with v' and J' we also displayed the energy value E obtained by the fit for the upper level of each series expressed relative to the ground state of that isotopomer. (In fact, the program returns the upper levels relative to the $v = 0$, $J = 0$ level of the reference isotopomer and therefore had to be corrected for the difference in zero-point energy for $^{79,81}Br_2$ and $^{81}Br_2$.) To check the validity of our calibration, we used the

TABLE 3—*Continued*

$^{79,81}Br_2$

v''	R	P
	$v'=15,\ J'=63,$	**E=18099.703(2)**
10	14683.221(-1)	14663.529(2)
11	14385.487(-10)	14365.881(-9)
13	13796.935(-10)	13777.502(-9)
14	13506.158(-4)	13486.818(-8)
16	12931.689(31)	12912.556(-3)
17	12648.105(-4)	12629.020(3)
19	12088.169(-2)	12069.232(40)
20	11811.907(-4)	11793.101(-2)
22	11266.895(9)	11248.277(11)
24	10732.122(13)	10713.697(12)
26	10207.840(-6)	10189.611(-6)
27	9949.684(7)	9931.604(-42)
29	9441.602(-2)	9423.657(16)
	$v'=12,\ J'=34,$	**E=17614.181(1)**
4	16253.119(-1)	16242.134(-3)
5	15940.992(-2)	15930.052(-4)
8	15017.888(-2)	15007.083(-3)
11	14115.022(0)	14104.356(-2)
12	13818.640(2)	13808.019(1)
13	13524.578(1)	13514.005(-1)
14	13232.843(7)	13222.328(-6)
15	12943.475(2)	12932.996(1)
16	12656.475(4)	12646.045(2)
18	12089.695(1)	12079.363(-1)
19	11809.955(1)	11799.670(1)
21	11257.900(-1)	11247.715(0)
22	10985.635(0)	10975.502(0)
23	10715.919(-2)	10705.835(0)
24	10448.781(-8)	10438.739(4)
25	10184.235(-1)	10174.257(0)
26	9922.332(1)	9912.411(-3)
28	9406.573(1)	9396.756(2)
29	9152.784(5)	9143.029(-1)
	$v'=10,\ J'=43,$	**E=17401.418(1)**
4	15985.909(-2)	15972.063(-4)
6	15364.296(2)	15350.565(-1)
8	14751.569(-2)	14737.956(-8)
9	14448.571(-1)	14435.010(-4)
10	14147.838(-1)	14134.335(-3)
12	13553.233(6)	13539.853(-1)
13	13259.407(1)	13246.079(2)
14	12967.911(4)	12954.644(3)
16	12392.015(5)	12378.870(2)
17	12107.663(-3)	12094.576(-3)
20	11269.195(4)	11256.299(1)
21	10994.664(2)	10981.827(4)
23	10453.196(-5)	10440.490(-4)
24	10186.306(-1)	10173.662(3)
25	9922.014(14)	9909.458(-3)
27	9401.436(-11)	9388.981(6)
	$v'=15,\ J'=54,$	**E=18047.417(2)**
6	15926.963(-2)	15909.771(-8)
10	14711.897(-1)	14694.999(-12)
11	14413.808(-6)	14396.965(0)
13	13824.538(1)	13807.849(3)
14	13533.410(-1)	13516.792(4)
16	12958.254(-5)	12941.785(2)
17	12674.257(4)	12657.876(0)
19	12113.574(7)	12097.354(-3)
20	11836.938(-2)	11820.783(4)
22	11291.162(7)	11275.179(1)
23	11022.103(-2)	11006.196(-3)
25	10491.738(2)	10475.998(0)
26	10230.508(2)	10214.853(-1)
27	9971.967(-8)	9956.358(29)
28	9716.120(1)	9700.611(24)
29	9463.031(3)	9447.633(2)
	$v'=16,\ J'=9,$	**E=18012.864(3)**
10	14893.937(1)	14890.993(-7)
11		14591.960(7)
13	14003.748(3)	14000.854(-17)
16	13134.567(-5)	13131.689(-1)
22		11458.658(-1)
25	10658.873(-12)	10656.100(12)
28		9877.262(4)
	$v'=15,\ J'=32,$	**E=17952.859(2)**
10	14762.470(3)	14752.398(-19)
11	14463.756(-4)	14453.696(5)
13	13873.222(-3)	13863.263(-7)
14	13581.443(3)	13571.542(-13)
16	13005.009(-24)	12995.153(5)
17	12720.336(2)	12710.559(-2)
20	11880.996(6)	11871.347(13)
22	11333.848(12)	11324.309(4)
23	11064.102(-9)	11054.584(10)
26	10270.353(6)	10261.016(-6)
29	9500.665(-4)	9491.461(6)
	$v'=12,\ J'=12,$	**E=17560.737(2)**
5	15966.070(-3)	15962.105(-4)
8	15042.001(-9)	15038.078(-4)
9	14738.432(7)	14734.532(7)
11	14138.151(-12)	14134.266(5)
12	13841.427(-3)	13837.573(-1)
15	12965.240(0)	12961.437(4)
16	12677.886(11)	12674.100(15)
18	12110.396(18)	12106.677(-9)
19	11830.311(9)	11826.594(-4)
22	11004.910(4)	11001.238(2)
24	10467.328(-18)	10463.673(0)
25	10202.390(3)	10198.780(-5)
	$v'=13,\ J'=42,$	**E=17764.629(2)**
7		15413.272(-5)
8	15121.361(-6)	15108.050(-4)
9	14818.328(1)	14805.086(-9)
11	14219.091(0)	14205.951(2)
12	13922.913(0)	13909.832(1)
14	13337.532(0)	13324.565(4)
15	13048.363(4)	13035.462(0)
16		12748.735(-3)
17		12464.400(2)
18	12195.219(1)	12182.493(0)
21	11364.069(5)	11351.533(0)
22	11092.032(0)	11079.556(-3)
24	10555.620(-1)	10543.268(2)
25	10291.307(3)	10279.019(5)
	$v'=10,\ J'=31,$	**E=17353.777(1)**
3	16322.383(-2)	16312.324(-16)
4	16008.006(-4)	15997.969(0)
8	14772.521(-2)	14762.651(0)
9	14469.233(-2)	14459.405(-1)
10	14168.206(1)	14158.422(0)
12	13573.013(5)	13563.311(7)
13	13278.889(-1)	13269.232(0)
14	12987.095(0)	12977.481(0)
16	12410.584(6)	12401.062(3)
17	12125.920(1)	12116.437(3)
19	11563.860(2)	11554.460(11)
20	11286.518(1)	11277.170(3)
21	11011.670(-3)	11002.363(4)
23	10469.544(-3)	10460.336(-2)
24	10202.327(-2)	10193.167(-1)
25	9937.731(-19)	9928.593(9)
27	9416.423(7)	9407.422(-5)
	$v'=13,\ J'=52,$	**E=17812.919(1)**
4	16330.098(-6)	16313.386(1)
5	16018.458(1)	16001.814(8)
7	15401.848(-22)	15385.323(3)
8	15096.860(-4)	15080.428(-2)
9	14794.142(-3)	14777.785(-7)
10	14493.677(12)	
11	14195.523(1)	14179.308(-4)
12	13899.659(2)	13883.505(7)
14	13314.913(3)	13298.912(-1)
15	13026.078(-4)	13010.143(-2)
18	12173.905(4)	12158.194(4)
21	11343.768(7)	11328.291(1)
22	11072.079(-3)	11056.668(3)
24	10536.361(2)	10521.117(-1)
25	10272.410(-2)	10257.237(5)
27	9752.470(-7)	9737.467(-6)
28	9496.542(0)	9481.622(1)

Gerstenkorn *et al.* (*22*) constants to calculate the term values of the observed levels of the $B^3\Pi_{0^+u}$ state. Very good agreement (to within a few 10^{-3} cm^{-1}) was observed between the E values returned by the fit and the calculated term values. In the case of the $^{79}Br_2$ ground state term values used in the fit, the position of the virtual level (20 000 cm^{-1}) introduced for the sake of data compatibility was found by the fit (20 000.00001(25) cm^{-1}) to well within the estimated uncertainty of Gerstenkorn *et al.* (*22*). The $^{79}Br_2$ $X^1\Sigma_g^+$ (v'' = 0–14, J'' = 0–100) term values introduced in the fit were reproduced by our constants within the estimated uncertainty of 0.002 cm^{-1}. However, a systematic deviation was observed between the "input" and the "output" term values, but this deviation was always much less than 0.002 cm^{-1}.

TABLE 3—*Continued*

$^{79,81}Br_2$

v''	R	P
	v'=17, J'=66,	E=18323.886(2)
9	15177.539(0)	15156.833(1)
10	14877.638(-2)	14857.022(-2)
12	14284.721(-6)	14264.275(3)
13	13991.736(-5)	13971.389(-2)
15		13392.649(7)
16	13126.930(-3)	13106.860(-2)
19	12283.780(4)	12263.998(3)
21	11734.041(-5)	
22	11462.949(-5)	11443.450(3)
23		11175.040(-22)
24	10928.456(7)	10909.174(-2)
25	10665.133(2)	10645.947(-1)
	v'=12, J'=62,	E=17754.061(2)
4	16181.372(-5)	16161.480(12)
8	14949.611(-4)	14930.058(1)
9	14647.268(-3)	14627.798(2)
12	13753.938(-11)	13734.711(4)
15		12862.552(-1)
19	11751.740(12)	11733.128(23)
22	10930.349(3)	10912.025(2)
25	10131.965(1)	10113.927(-2)
26	9871.096(-3)	9853.156(-7)
	v'=13, J'=36,	E=17740.501(2)
4	16368.439(10)	16356.830(-4)
5	16056.379(-13)	16044.797(-7)
8	15133.403(-5)	15121.971(-5)
9	14830.225(-7)	14818.838(-4)
11	14230.674(-2)	14219.387(-1)
12	13934.332(6)	13923.091(10)
14	13348.642(-1)	13337.507(-3)
15	13059.313(2)	13048.229(0)
17	12487.809(6)	12476.823(8)
18	12205.678(2)	12194.743(5)
21	11374.035(-2)	11363.255(4)
22	11101.809(11)	11091.094(6)
24	10565.061(0)	10554.453(-2)
25	10300.573(2)	10290.016(5)
27	9779.549(-1)	9769.102(6)
28	9523.082(-5)	9512.690(3)
	v'=11, J'=40,	E=17514.690(2)
3	16432.937(-1)	16419.992(-2)
4	16118.761(-2)	16105.867(-2)
5	15806.765(7)	
6	15496.989(2)	15484.207(-6)
8	14884.101(-2)	14871.416(-1)
9	14581.020(-1)	14568.391(-2)
10	14280.200(5)	14267.635(-5)
12	13685.436(5)	13672.976(-1)
	v'=19, J'=108,	E=18845.209(3)
3	16966.658(1)	16932.161(-2)
4	16655.706(1)	16621.342(4)
6	16040.441(2)	16006.372(-6)
9	15134.398(-16)	15100.739(-1)
10	14836.893(23)	
	v'=15, J'=62,	E=18093.510(3)
5	16209.543(5)	16189.769(-15)
7	15593.652(2)	15574.023(1)
8	15289.057(0)	15269.506(2)
10	14686.643(-1)	14667.262(-2)
11	14388.853(3)	14369.557(1)
	v'=15, J'=80,	E=18219.729(2)
7		15495.478(-21)
8		15191.807(-3)
10	14616.226(-2)	14591.295(0)
11	14319.296(-3)	14294.472(2)
13	13732.390(-4)	13707.785(2)
14	13442.444(3)	13417.960(-2)
16	12869.688(9)	12845.439(-5)
17	12586.930(1)	12562.779(3)
19		12004.801(9)
20	11753.333(7)	11729.538(1)
21	11480.459(4)	11456.768(13)
22	11210.127(-3)	
23	10942.351(1)	10918.906(3)
24	10677.178(-4)	10653.858(-2)
26	10154.737(0)	10131.672(-5)
27	9897.552(-9)	9874.601(-3)
29	9391.386(-3)	9368.723(-27)
	v'=11, J'=59,	E=17613.816(2)
8	14837.517(0)	14818.903(0)
9	14535.055(0)	14516.520(0)
10	14234.854(7)	14216.419(-13)
12	13641.349(4)	13623.053(6)
13	13348.073(1)	13329.866(-5)
15	12768.538(22)	
16	12482.370(-5)	12464.399(1)
17		12180.686(8)
19	11638.294(1)	11620.579(6)
20	11361.850(5)	11344.233(-3)
22	10816.498(2)	10799.058(-7)
23	10547.639(2)	10530.276(4)
26	9756.686(7)	9739.608(-3)
27		9481.378(-11)
	v'=11, J'=29,	E=17474.412(3)
4	16138.029(3)	16128.634(2)
8	14902.394(2)	14893.160(-6)
9	14599.074(-6)	14589.864(2)
	v'=12, J'=39,	E=17633.276(2)
4	16243.556(-2)	16230.988(-10)
5	15931.548(-5)	15919.026(-9)
8	15008.791(1)	14996.421(0)
9	14705.675(11)	14693.356(12)
11	14106.287(1)	14094.086(-10)
12	13810.020(9)	13797.873(-2)
15	12935.226(9)	12923.234(5)
16	12648.345(18)	12636.413(9)
19	11802.232(-9)	11790.447(3)
21	11250.428(1)	11238.789(-18)
22	10978.300(-3)	10966.702(-4)
25	10177.310(-6)	10165.889(-6)
26	9915.548(-8)	9904.168(14)
	v'=13, J'=19,	E=17691.975(2)
8	15156.783(-6)	15150.667(-1)
9	14853.296(-3)	14847.216(-7)
11	14253.134(-1)	14247.102(-2)
12	13956.488(1)	13950.487(-5)
13	13662.124(36)	
14	13370.153(11)	13364.209(2)
15	13080.520(2)	13074.603(-8)
17	12508.362(14)	12502.501(3)
18		12220.094(-21)
21	11393.271(3)	11387.514(1)
24	10583.277(-2)	10577.602(1)
25	10318.441(-3)	10312.803(-7)
27	9796.693(7)	9791.111(6)
28		9534.320(-7)
	v'=12, J'=50,	E=17684.310(1)
4	16217.557(-4)	16201.484(-1)
8	14984.057(-3)	14968.252(-4)
9	14681.275(-6)	14665.533(-3)
11	14082.523(-4)	14066.912(4)
12	13786.588(0)	13771.055(-2)
13	13492.988(-10)	13477.515(-4)
15	12912.792(0)	12897.462(3)
16	12626.251(7)	12610.995(5)
18	12060.421(-6)	12045.295(5)
19	11781.143(7)	11766.105(4)
21	11230.063(-3)	11215.161(5)
22	10958.288(-1)	10943.465(2)
23	10689.067(-3)	10674.323(-3)
25	10158.392(-2)	10143.798(1)
26	9897.003(-2)	9882.487(2)
28	9382.284(3)	
	v'=22, J'=28,	E=18606.343(3)
5	16962.163(13)	16953.126(9)
8	16038.712(1)	16029.790(-6)
11	15135.494(-11)	15126.676(-8)

IV. DISCUSSION

Looking at Table 2 it is interesting to note that although our data extended to $v'' = 29$, we needed shorter (by one unit) expansions for B_v's, and D_v's than did Gerstenkorn *et al.* (*22*). Also we did not need to add H_v parameters in order to reproduce our data to within the experimental precision. However, we did need to use a higher order (by one unit) expansion for the G_v parameters. It should be noted, though, that the centrifugal distortion constants (CDCs) in the study of Gerstenkorn *et*

TABLE 3—*Continued*

$^{79,81}Br_2$

v''	R	P
	$v'=11$, $J'=51$,	E=17567.533(2)
8	14859.449(3)	14843.337(-4)
9	14556.701(-1)	14540.651(-1)
10	14256.212(4)	
12	13662.124(-4)	13646.281(-3)
13	13368.536(7)	13352.770(1)
16	12501.937(-9)	
17		12202.310(34)
18		11920.781(-39)
19	11656.943(-16)	
20		11364.903(3)
22	10834.165(8)	
23	10564.981(6)	10549.964(-11)
26	9773.027(12)	9758.247(-7)
27	9514.371(-5)	
	$v'=18$, $J'=13$,	E=18220.830(2)
4	16936.701(-5)	
5	16624.258(-3)	
6	16314.018(-1)	16309.755(-4)
7	16005.993(3)	16001.755(-8)
9	15396.661(-1)	15392.449(-2)
10	15095.375(3)	15091.184(-1)
12	14499.663(5)	14495.507(3)
13	14205.276(0)	14201.129(7)
15	13623.508(1)	13619.406(-1)
16	13336.168(6)	13332.096(-6)
18	12768.703(6)	12764.666(-4)
21	11935.860(4)	11931.873(4)
	$v'=11$, $J'=81$,	E=17774.947(2)
4	15987.893(8)	15962.037(-16)
8	14759.678(-7)	14734.225(-7)
9	14458.225(-1)	14432.889(-9)
13	13275.383(-3)	13250.467(10)
20	11296.724(7)	11272.628(9)
23	10485.927(-6)	10462.178(12)
	$v'=10$, $J'=18$,	E=17319.327(2)
2	16654.557(22)	
3	16337.832(-8)	16331.902(5)
4	16023.247(-2)	16017.352(-1)
6	15400.664(0)	15394.821(-3)
8	14786.955(-6)	14781.144(7)
9	14483.455(-1)	14477.681(0)
10	14182.222(0)	14176.475(-1)
11		13877.528(18)
12		13580.906(9)
	$v'=15$, $J'=6$,	E=17902.585(4)
3	16943.151(6)	16941.073(4)
4	16628.489(-1)	16626.418(-1)
10	14786.931(-9)	

v''	R	P
	$v'=11$, $J'=43$,	E=17527.851(2)
8	14878.004(-3)	14864.384(-4)
9	14575.002(0)	14561.442(-2)
10	14274.266(4)	14260.766(0)
12	13679.674(-2)	13666.281(3)
13	13385.843(-1)	13372.503(10)
16	12518.442(11)	12505.295(10)
19	11672.655(3)	11659.698(-2)
20	11395.632(0)	11382.737(-4)
22	10849.093(-5)	10836.318(-1)
23	10579.628(-4)	10566.918(1)
26	9786.826(-3)	9774.330(-14)
	$v'=15$, $J'=26$,	E=17935.324(2)
3	16926.311(3)	16917.845(-6)
4	16611.849(-4)	16603.407(-4)
5		16291.145(12)
6	15989.451(35)	15981.120(-6)
8	15376.002(-5)	15367.701(-7)
10	14771.498(1)	14763.268(-2)
11	14472.659(3)	14464.461(3)
13	13881.902(-5)	13873.778(-6)
14	13590.007(0)	13581.921(-3)
16	13013.309(0)	
17	12728.528(14)	12720.564(-1)
20		11880.969(5)
	$v'=14$, $J'=59$,	E=17966.126(2)
4	16422.057(0)	16403.133(-1)
5		16091.827(-2)
6	15801.495(2)	
7	15494.542(1)	15475.849(1)
8	15189.827(0)	15171.214(-1)
9	14887.365(0)	14868.834(-4)
10	14587.175(-3)	14568.717(0)
11	14289.267(-1)	14270.890(0)
12	13993.659(5)	13975.364(5)
14	13409.451(-5)	
	$v'=14$, $J'=58$,	E=17960.236(2)
4	16425.392(-1)	16406.780(3)
5	16113.970(0)	16095.439(-2)
7	15497.778(-14)	15479.384(1)
8	15193.013(-3)	15174.709(-1)
10	14590.277(0)	14572.129(2)
11	14292.334(-2)	14274.267(-2)
13		13685.436(28)
	$v'=22$, $J'=24$,	E=18597.063(3)
5	16969.075(1)	16961.301(2)
6	16658.965(1)	16651.225(0)
8	16045.420(-7)	16037.739(-2)
11	15141.979(1)	15134.398(3)

v''	R	P
	$v'=12$, $J'=52$,	E=17694.902(2)
8	14978.846(-6)	14962.409(0)
9	14676.138(-16)	14659.766(-5)
11		14061.280(7)
12	13781.646(-2)	13765.487(8)
13	13488.105(-3)	
15	12908.056(1)	
16		12605.731(3)
21	11225.756(2)	
22	10954.052(7)	10938.653(2)
25	10154.402(-11)	10139.222(2)
	$v'=14$, $J'=82$,	E=18128.771(2)
8	15100.851(-5)	15075.089(-6)
10	14500.332(6)	14474.799(-3)
11	14203.517(-1)	14178.088(-3)
12	13909.010(-3)	13883.691(-2)
14	13326.998(3)	13301.908(0)
15	13039.550(-8)	13014.566(-1)
17	12471.821(3)	
18	12191.606(1)	12166.978(3)
20	11638.573(8)	11614.172(22)
21	11365.821(2)	11341.553(4)
23	10827.947(5)	10803.930(3)
24	10562.898(0)	10539.006(-2)
26		10017.075(-5)
27	9783.642(-1)	9760.136(-4)
28	9529.309(-4)	
	$v'=13$, $J'=5$,	E=17674.100(2)
4	16400.804(-4)	16399.049(-2)
5	16088.317(-2)	16086.566(5)
7		15468.238(-3)
8	15164.126(5)	15162.408(0)
9	14860.540(1)	14858.831(-6)
11	14260.166(-1)	14258.458(6)
12	13963.409(4)	13961.716(3)
	$v'=11$, $J'=54$,	E=17584.106(2)
3	16398.340(-7)	16380.923(-1)
4	16084.574(0)	16067.234(0)
6	15463.653(-3)	15446.455(-2)
8	14851.617(-3)	14834.558(0)
9	14548.965(0)	14531.983(0)
10	14248.581(4)	14231.677(-2)
12	13654.693(6)	13637.937(-1)
13	13361.233(-5)	13344.530(11)
	$v'=12$, $J'=64$,	E=17767.102(3)
4	16174.534(0)	16154.023(1)
8	14943.102(-2)	14922.932(-2)
9	14640.835(5)	14620.755(0)

al. (*22*) are actually calculated in a self-consistent manner from a corrected RKR (Rydberg-Klein-Rees) potential energy curve and not directly fitted to the experimental data. This could explain the small systematic deviation observed between the $^{79}Br_2$ $X^1\Sigma_g^+$ (v'' = 0–14, J'' = 0–100) ground state term values computed using the two sets of constants.

Our constants are in very good agreement with those of Gerstenkorn *et al.* (*22, 23*) for the first k's of the $Y_{k,m}$ expansions (see Table 2 of the present work, Table V of Ref. (*22*), and Tables VII, VIII, and IX of Ref. (*23*)): for instance, the $Y_{1,0}$ (ω_e) parameters agree within 5×10^{-4} cm^{-1}, and the $Y_{0,1}$ (B_e) parameters agree within 3×10^{-7} cm^{-1}. However, for higher k values ($k = 5$ for $m = 0$ or $k = 2$ for $m = 2$) this agreement deteriorates, although the corresponding values remain of the

TABLE 3—*Continued*

$^{79,81}Br_2$

v''	R	P	v''	R	P	v''	R	P
	$v'=12$, $J'=56$,	E=17717.359(2)		$v'=16$, $J'=47$,	E=18118.452(2)		$v'=14$, $J'=27$,	E=17826.573(3)
4	16200.487(1)	16182.513(2)	6	16053.233(0)	16038.240(-1)	5	16186.687(2)	16177.964(1)
5	15888.988(5)	15871.094(-1)	8	15440.739(-3)	15425.866(0)	7	15568.781(4)	15560.134(-2)
7	15272.639(1)	15254.889(-2)	9	15137.855(0)	15123.047(1)	8	15263.174(-1)	15254.556(1)
8	14967.813(-2)	14950.133(0)	10	14837.242(0)	14822.497(1)	10	14658.710(-1)	14650.165(1)
9	14665.235(0)	14647.629(2)	11	14538.911(1)	14524.236(-4)	11	14359.888(1)	14351.389(-6)
11	14066.916(-9)	14049.451(4)	13	13949.170(5)	13934.620(4)			
			14		13643.323(-5)			

$^{81}Br_2$

v''	R	P	v''	R	P	v''	R	P
	$v'=12$, $J'=20$,	E=17565.588(1)		$v'=12$, $J'=26$,	E=17580.002(2)		$v'=13$, $J'=67$,	E=17892.561(2)
4	16271.831(-6)	16265.384(-9)	4	16264.992(10)	16256.683(-17)	5	15971.989(-1)	15950.885(-4)
5	15961.349(-3)	15954.924(-2)	5	15954.614(-5)	15946.307(-1)	8	15057.557(-11)	15036.708(-8)
8	15043.015(-4)	15036.672(-7)	8	15036.530(3)	15028.329(3)	9	14757.164(1)	14736.410(-3)
9	14741.326(-11)	14734.997(0)	11	14138.436(-8)	14130.334(-3)	11	14163.152(-6)	14142.578(-12)
11	14144.639(2)	14138.372(4)	12	13843.564(8)	13835.510(0)	12	13869.552(-9)	13849.041(11)
12	13849.696(0)	13843.458(0)	13	13551.034(-32)	13542.975(1)	14	13289.244(-6)	13268.883(45)
13	13557.032(3)	13550.818(6)	15	12972.797(-7)	12964.840(-5)	15	13002.561(14)	12982.361(-4)
15	12978.637(4)	12972.484(2)	16	12687.174(13)	12679.266(2)	18	12156.781(7)	12136.853(-1)
16	12692.948(-2)	12686.814(5)	19	11844.653(-7)	11836.841(-3)	19	11879.654(14)	11859.828(-1)
18	12128.659(6)	12122.582(13)	21	11295.039(30)	11287.326(10)	21	11332.787(-3)	11313.129(7)
19	11850.126(-3)	11844.078(3)	22	11023.983(5)	11016.285(9)	22	11063.066(5)	11043.512(9)
21	11300.364(-11)	11294.364(6)	25	10225.910(2)	10218.342(-8)	24	10531.239(2)	10511.892(-2)
22	11029.176(-1)	11023.221(1)	26	9965.038(0)	9957.500(2)	25	10269.189(-5)	10249.931(3)
23	10760.507(-2)	10754.592(-10)				28	9498.813(9)	9479.894(-9)
25	10230.800(-1)	10224.935(2)		$v'=13$, $J'=26$,	E=17698.998(2)			
26	9969.826(-1)	9963.990(3)	7		15451.115(6)		$v'=13$, $J'=34$,	E=17723.584(1)
28	9455.790(2)	9450.019(5)	8	15155.531(-2)	15147.329(-1)	4	16371.450(16)	16360.619(-4)
			9	14853.926(-5)	14845.748(6)	5	16061.225(-3)	16050.417(-2)
	$v'=13$, $J'=63$,	E=17866.334(2)	10		14546.394(21)	8	15143.604(-3)	15132.930(-3)
5	15986.109(-3)	15966.246(-1)	11	14257.425(-1)	14249.329(-2)	9	14842.143(3)	14831.514(3)
8	15071.172(-5)	15051.552(-1)	12	13962.566(3)	13954.510(-4)	11	14245.957(2)	14235.423(-3)
9	14770.623(-5)	14751.091(-7)	14	13379.729(2)	13371.737(2)	12	13951.257(2)	13940.767(-1)
11	14176.259(0)	14156.890(3)	15	13091.783(2)	13083.831(0)	14	13368.739(-1)	13358.338(0)
12	13882.485(-1)	13863.206(-4)	17	12522.942(2)	12515.071(-9)	15	13080.953(1)	13070.598(2)
14	13301.826(6)	13282.718(3)	18	12242.087(2)	12234.241(3)	17	12512.420(16)	
15	13014.992(1)	12995.969(0)	19	11963.648(-6)		18	12231.754(-9)	12221.533(2)
18	12168.687(-15)	12149.904(6)	20		11679.855(0)	19	11953.463(1)	11943.286(16)
21	11344.113(3)	11325.626(0)	21	11414.066(-2)	11406.330(2)	21	11404.218(4)	11394.157(1)
22	11074.205(10)	11055.807(10)	22	11142.985(0)	11135.303(-13)	22	11133.317(-4)	11123.301(-2)
24	10542.002(3)	10523.790(4)	23	10874.407(6)		24	10599.054(-1)	10589.145(-5)
25	10279.748(6)	10261.641(-2)	24	10608.383(-6)	10600.763(-3)	25	10335.759(1)	10325.907(-8)
						27	9817.009(-7)	9807.245(0)
	$v'=13$, $J'=40$,	E=17746.246(2)		$v'=13$, $J'=33$,	E=17720.164(2)	28	9561.604(-1)	9551.902(-1)
4	16359.692(0)	16346.957(0)	4	16373.233(2)	16362.702(-3)			
5	16049.586(1)	16036.906(-3)	5	16062.976(-5)	16052.480(-3)		$v'=12$, $J'=9$,	E=17548.716(3)
7	15435.921(-2)	15423.339(1)	7	15448.976(5)	15438.573(0)	4	16279.179(3)	16276.191(2)
8	15132.390(-3)	15119.859(0)	8	15145.287(-1)	15134.922(-1)	5	15968.605(1)	15965.629(-1)
9	14831.073(1)	14818.603(-4)	11	14247.573(6)	14237.344(2)	7	15353.958(29)	15351.048(-14)
11	14235.170(4)	14222.807(-1)	12	13952.856(2)		9	14748.182(-3)	14745.249(1)
12	13940.611(9)	13928.307(-1)				12	13856.244(12)	13853.373(-8)

same order of magnitude. The explanation of this behavior lies in the different orders used in the Dunham expansion, the use of calculated CDCs by Gerstenkorn *et al.*, and in the fact that we expanded the v'' range from $v''=0$–14 to $v''=0$–29. Our empirical Dunham parameters are to be regarded as a minimal set of experimentally determined constants that reproduce both our new fluorescence data and the existing ground state energy levels of Gerstenkorn *et al.*

We also undertook a comparative study between our work and that of Venkateswarlu *et al.* (*32*). Those authors recorded 12 fluorescence series (in the region 1500–2000 Å) excited by four atomic bromine lines using the 10.7-m vacuum spectro-

TABLE 3—*Continued*

$^{81}Br_2$

v''	R	P
	$v'=16,\ J'=58,$	**E=18163.257(2)**
9	15113.693(1)	
10	14815.190(-1)	14797.267(-3)
11	14518.949(-8)	14501.101(-8)
13	13933.284(0)	13915.588(4)
14	13643.921(-10)	13626.299(-1)
16	13072.175(0)	13054.715(7)
17	12789.842(11)	12772.481(0)
19	12232.410(0)	12215.199(3)
20	11957.337(-1)	11940.204(7)
22	11414.615(-5)	11397.657(-3)
23	11147.014(-5)	11130.141(-2)
25	10619.476(4)	10602.787(-2)
26	10359.616(-4)	10343.005(1)
28	9847.841(-6)	9831.400(8)
29	9596.003(-9)	9579.650(10)
	$v'=10,\ J'=9,$	**E=17298.372(3)**
3	16341.588(-13)	16338.569(5)
4	16028.844(-5)	16025.851(-2)
6	15409.855(4)	15406.903(-10)
9	14497.833(2)	14494.904(2)
10	14198.257(15)	14195.355(0)
	$v'=14,\ J'=18,$	**E=17796.186(3)**
5	16197.739(3)	16191.940(4)
7	15583.260(13)	
8	15279.338(-3)	15273.611(-2)
9	14977.642(-26)	
10		14672.461(-10)
11	14380.888(5)	14375.237(2)
	$v'=15,\ J'=61,$	**E=18075.650(3)**
5	16214.658(3)	16195.418(5)
7	15602.339(0)	15583.265(-8)
8	15299.484(0)	15280.485(-2)
10	14700.467(-2)	14681.625(0)
11	14404.336(-1)	14385.571(4)
	$v'=14,\ J'=49,$	**E=17900.838(3)**
5	16142.178(3)	16126.685(1)
7	15529.021(1)	15513.657(-4)
8	15225.746(-1)	15210.440(0)
10	14625.878(-6)	14610.697(0)
11	14329.304(6)	14314.197(3)
	$v'=17,\ J'=23,$	**E=18128.430(3)**
6	16206.053(-1)	16198.717(1)
9	15294.451(-3)	15287.203(2)
10	14995.023(4)	14987.819(-4)
13	14110.327(7)	14103.220(-4)
	$v'=12,\ J'=60,$	**E=17730.700(3)**
4	16188.573(-1)	16169.569(0)
8	14963.802(2)	14945.112(-1)
9	14663.137(-1)	14644.521(0)
11		14050.064(17)
	$v'=17,\ J'=28,$	**E=18140.783(3)**
6	16198.904(-3)	16190.013(-4)
9	15287.538(1)	15278.754(3)
10	14988.208(-8)	14979.456(-1)
13	14103.755(1)	14095.115(9)
	$v'=15,\ J'=98,$	**E=18361.765(3)**
4	16351.849(-8)	16321.001(-2)
7	15435.694(2)	15405.232(1)
8	15134.734(3)	15104.399(2)
10	14539.544(3)	

graph of the National Research Council in Ottawa. They claimed that their data involved the $v'' = 0$–76 vibrational levels of the $X^1\Sigma_g^+$ ground state of $^{79,81}Br_2$. The precision of their measurements was about 0.06 cm^{-1} and they based the assignment of their fluorescence series on the $v'' = 0$–10 rotational and vibrational constants available at that time (*20*). In the 1982 paper they changed the assignment of one fluorescence series, previously recorded (*30*), from $J' = 62$ to $J' = 58$. Our new high-resolution measurements gave us the opportunity to check the assignments of Venkateswarlu *et al.* (*32*), because among the 12 fluorescence series they reported, 6 have some common lower levels with fluorescence series that we recorded. We compared the $\Delta\nu_{RP}$ differences between the wavenumbers of the *R* and *P* lines for given v'' levels and the agreement was always on the order of their estimated uncertainty (a maximum deviation of 0.15 cm^{-1} was observed). This seems to validate their assignment for these six fluorescence progressions. However, when we tried to reproduce our data using the rovibrational constants they provide (which are supposed to be valid up to $v'' = 76$; see Table IX of Ref. (*32*)), a very large discrepancy was observed (the dimensionless rms discrepancy with our data was more than 200). The calculated and observed data are more or less satisfactory at low v'' values (typically $v'' < 10$) but this agreement rapidly deteriorates as v'' increases, yielding calculated − observed differences of about 15 cm^{-1} at $v'' = 29$. In the future we intend to make our own independent analysis of the high-vibrational levels of the ground state of Br_2 using a new high-purity Ge detector to work in the near infrared.

Another comparison can be made with the more recent fluorescence study of Franklin *et al.* (*24*). They recorded more than 100 bandheads which involved the $v'' = 1$–27 levels of the ground state of the $^{79,81}Br_2$ isotopomer. However, their spectra were only vibrationally resolved, and the vibrational constants they reported are much less accurate than ours (for instance, $\omega_e = 323.88 \pm 0.74$ cm^{-1} (*24*) compared to $\omega_e = 323.2998 \pm 0.0003$ cm^{-1} in our work).

Several authors have calculated RKR potential curves for the $X^1\Sigma_g^+$ ground state of Br_2, using various sets of spectroscopic constants. Le Roy and Burns (*31*) used the constants of Rao and Venkateswarlu (*30*) (whose rotational assignment was wrong) to obtain an RKR potential curve up to $v'' = 36$. Later, Coxon used the data of Horsley and Barrow (*15*) and his own data (*17*) up to $v'' = 10$, and again used the vibrational part of the fluorescence data of Rao and Venkateswarlu (*30*) for $v'' = 11$–36 to calculate the RKR potential curve for the $X^1\Sigma_g^+$ ground state as well as Franck–Condon factors and *r*-centroids for the $B^3\Pi_{0^+u}$–$X^1\Sigma_g^+$ system (*18, 19*). Then Barrow *et al.* (*20*) used their improved constants for $v'' = 0$–10 to derive an RKR potential curve for the ground state and Franck–Condon factors and *r*-centroids for the *B*–*X* system. Finally, in 1987, Gerstenkorn *et al.* (*22, 23*) built a corrected RKR (an IPA potential) curve of the ground state and derived Franck–Condon factors from the analysis of their high-resolution FTS absorption spectrum of the *B*–*X* system (including the $v'' = 0$–14 and $v' = 0$–52 vibrational levels).

As our measurements extend the range of the high-resolution data available for the ground state to $v'' = 0$–29, we decided to

calculate the RKR potential energy curve of this state, using the B_v (Y_{k1}) and G_v (Y_{k0}) expansion parameters of $^{79}Br_2$ listed in Table 4. Figure 3 shows the potential curve we obtained for the ground state (limited to the observed vibrational levels, $v'' \leq 29$). For the common range $0 \leq v'' \leq 14$, our turning points are in excellent agreement ($\leq 3 \times 10^{-6}$ Å) with those calculated by Gerstenkorn *et al.* (*22*). The RKR turning points were generated with the program of R. J. Le Roy. The equilibrium internuclear distance, calculated from the usual relationship with B_e (*50*), was found to be $R_e = 2.2810213(20)$ Å. Taking into account the ground state dissociation energy (D_0) of 15 894.546(10) for $^{79}Br_2$ (*23*), we can observe from Figure 3 that this state is now known reliably about half way to dissociation.

V. CONCLUSION

The use of a Fourier transform spectrometer to record the laser-induced fluorescence spectrum of the $B^3\Pi_{0^+u}$–$X^1\Sigma_g^+$ system of Br_2 extends the high-resolution knowledge of the vibrational levels of the $X^1\Sigma_g^+$ ground state from $v'' \leq 14$ (*22*, *23*) to $v'' \leq 29$. We identified 1784 lines in 96 fluorescence progressions involving rovibrational levels of all three natural bromine isotopomers, in the range $10 \leq v' \leq 22$, $2 \leq v'' \leq 29$, and $4 \leq J'' \leq 109$. These data were merged with previous high-resolution FTS data for the $^{79}Br_2$ isotopomer (*22*) in a least-squares analysis to characterize the $X^1\Sigma_g^+$ ground state up to $v'' = 29$. An improved set of Dunham constants was derived and they describe the experimental data with a standard deviation of ~ 0.004 cm^{-1}. The B_v (Y_{k1}) and G_v (Y_{k0}) expansion parameters were used to calculate an RKR potential energy curve of this state up to $v'' = 29$, about halfway to dissociation.

TABLE 4
The Calculated RKR Turning Points of the Ground State of Br_2

v	G_v (cm^{-1})	B_v (cm^{-1})	R_{min} (Å)	R_{max} (Å)
0	162.3803	0.08194837	2.2317662	2.3344047
1	485.5306	0.08162622	2.1981020	2.3763768
2	806.5050	0.08130243	2.1760266	2.4068299
3	1125.2909	0.08097696	2.1587170	2.4325885
4	1441.8750	0.08064974	2.1441942	2.4556337
5	1756.2437	0.08032069	2.1315544	2.4768713
6	2068.3828	0.07998974	2.1202952	2.4968059
7	2378.2777	0.07965681	2.1101034	2.5157528
8	2685.9132	0.07932182	2.1007684	2.5339253
9	2991.2737	0.07898467	2.0921403	2.5514755
10	3294.3429	0.07864527	2.0841085	2.5685170
11	3595.1037	0.07830351	2.0765881	2.5851373
12	3893.5386	0.07795928	2.0695128	2.6014059
13	4189.6294	0.07761247	2.0628294	2.6173790
14	4483.3568	0.07726296	2.0564944	2.6331034
15	4774.7011	0.07691063	2.0504720	2.6486185
16	5063.6415	0.07655533	2.0447321	2.6639580
17	5350.1565	0.07619694	2.0392491	2.6791515
18	5634.2235	0.07583530	2.0340011	2.6942247
19	5915.8189	0.07547028	2.0289694	2.7092009
20	6194.9181	0.07510172	2.0241374	2.7241011
21	6471.4954	0.07472945	2.0194906	2.7389445
22	6745.5237	0.07435332	2.0150165	2.7537487
23	7016.9750	0.07397315	2.0107035	2.7685306
24	7285.8196	0.07358876	2.0065416	2.7833056
25	7552.0265	0.07319997	2.0025216	2.7980890
26	7815.5635	0.07280660	1.9986353	2.8128950
27	8076.3966	0.07240844	1.9948752	2.8277378
28	8334.4900	0.07200530	1.9912344	2.8426311
29	8589.8067	0.07159698	1.9877066	2.8575886

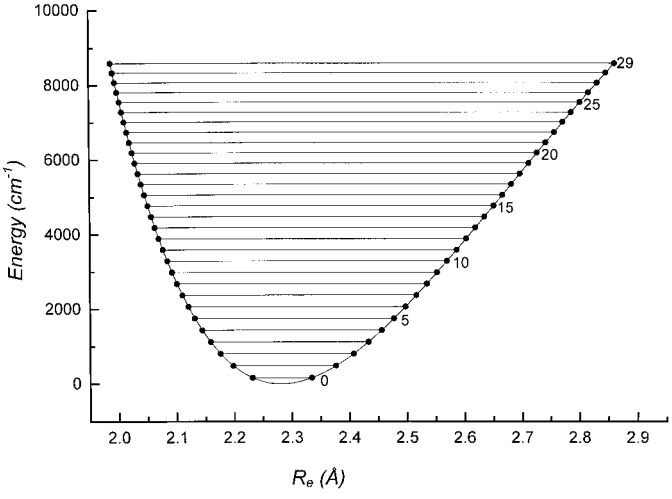

FIG. 3. RKR potential energy curve for the $X^1\Sigma_g^+$ ground state of Br_2, showing the vibrational levels experimentally observed in this work up to $v = 29$.

ACKNOWLEDGMENTS

This work was supported by the Natural Sciences and Engineering Research Council of Canada (NSERC). We thank Professor Robert J. Le Roy for making available to us the DSParFit program and for invaluable assistance in using it. C.F. thanks Professor Bernard Pinchemel for very useful discussions. We thank Professor Le Roy for his detailed comments on our manuscript.

REFERENCES

1. G. Capelle, K. Sakurai, and H. P. Broida, *J. Chem. Phys.* **54,** 1728–1730 (1971).
2. F. Zaraga, N. S. Nogar, and C. B. Moore, *J. Mol. Spectrosc.* **63,** 564–571 (1976).
3. K. B. McAfee, Jr. and R. S. Hozack, *J. Chem. Phys.* **64,** 2491–2495 (1976).
4. M. A. A. Clyne and M. C. Heaven, *J. Chem. Soc., Faraday Trans. 2* **74,** 1992–2013 (1978).
5. M. A. A. Clyne, M. C. Heaven, and E. Martinez, *J. Chem. Soc., Faraday Trans. 2* **76,** 405–419 (1980).
6. M. C. Heaven, *Chem. Soc. Rev.* **15,** 405–448 (1986).

7. F. J. Wodarczyk and H. R. Schlossberg, *J. Chem. Phys.* **67,** 4476–4482 (1977).
8. H. Kuhn, *Z. Phys.* **39,** 77–91 (1926).
9. W. G. Brown, *Phys. Rev.* **38,** 1179–1186 (1931).
10. W. G. Brown, *Phys. Rev.* **39,** 777–787 (1932).
11. R. S. Mulliken, *Phys. Rev.* **36,** 364 (1930).
12. R. S. Mulliken, *Phys. Rev.* **36,** 699–705 (1930).
13. R. S. Mulliken, *Phys. Rev.* **46,** 549–571 (1934).
14. O. Darbyshire, *Proc. R. Soc. London, Ser. A* **159,** 93–109 (1937).
15. J. A. Horsley and R. F. Barrow, *Trans. Faraday Soc.* **63,** 32–38 (1967).
16. M. A. A. Clyne and J. A. Coxon, *J. Mol. Spectrosc.* **23,** 258–271 (1967).
17. J. A. Coxon, *J. Mol. Spectrosc.* **37,** 39–62 (1971).
18. J. A. Coxon, *J. Quant. Spectrosc. Radiat. Transfer* **11,** 443–462 (1971).
19. J. A. Coxon, *J. Quant. Spectrosc. Radiat. Transfer* **12,** 639–650 (1972).
20. R. F. Barrow, T. C. Clark, J. A. Coxon, and K. K. Yee, *J. Mol. Spectrosc.* **51,** 428–449 (1974).
21. S. Gerstenkorn, P. Luc, and A. Raynal, "Atlas du Spectre d'Absorption de la Molecule de Brome," 2 vols., CNRS, Paris, 1985.
22. S. Gerstenkorn, P. Luc, A. Raynal, and J. Sinzelle, *J. Phys. (France)* **48,** 1685–1696 (1987).
23. S. Gerstenkorn and P. Luc, *J. Phys. (France)* **50,** 1417–1432 (1989).
24. R. E. Franklin, C. D. Holmberg, J. R. Reynolds, and G. P. Perram, *J. Mol. Spectrosc.* **184,** 273–276 (1997).
25. J. A. Horsley, *J. Mol. Spectrosc.* **22,** 469–470 (1967).
26. J. A. Coxon and M. A. A. Clyne, *J. Phys. B: At., Mol. Opt. Phys.* **3,** 1164–1165 (1970).
27. J. A. Coxon, *J. Mol. Spectrosc.* **41,** 548–565 (1972).
28. J. A. Coxon, *J. Mol. Spectrosc.* **41,** 566–576 (1972).
29. I. Mills, T. Cvitas, K. Homann, N. Kallay, and K. Kutchitsu, "Quantities, Units and Symbols in Physical Chemistry," 2nd ed.; Blackwell Scientific, Oxford, 1993.
30. Y. V. Rao and P. Venkateswarlu, *J. Mol. Spectrosc.* **13,** 288–295 (1964).
31. R. J. Le Roy and G. Burns, *J. Mol. Spectrosc.* **25,** 77–85 (1968).
32. P. Venkateswarlu, V. N. Sarma, and Y. V. Rao, *J. Mol. Spectrosc.* **96,** 247–265 (1982).
33. W. Holzer, W. F. Murphy, and H. J. Bernstein, *J. Chem. Phys.* **52,** 469–470 (1970).
34. S. H. Dworetsky and R. S. Hozack, *J. Chem. Phys.* **59,** 3856–3860 (1973).
35. R. M. Dworetsky and R. S. Hozack, *J. Mol. Spectrosc.* **58,** 325–327 (1975).
36. H. Chang and D.-M. Hwang, *J. Mol. Spectrosc.* **65,** 430–436 (1977).
37. R. S. Hozack, A. P. Kennedy, and K. B. McAfee, Jr., *J. Mol. Spectrosc.* **80,** 239–243 (1980).
38. G. De Vlieger, F. Claesens, and H. Eisendrath, *J. Mol. Spectrosc.* **83,** 339–342 (1980).
39. D. Cerny, R. Bacis, and J. Vergès, *J. Mol. Spectrosc.* **116,** 458–498 (1986).
40. B. Edlén, *Metrologia* **2,** 71–80 (1966).
41. K. P. Birch and M. J. Downs, *Metrologia* **30,** 155–162 (1993).
42. R. J. Le Roy, *J. Mol. Spectrosc.* **194,** 189–196 (1999).
43. R. J. Le Roy, *J. Mol. Spectrosc.* **191,** 223–231 (1998).
44. E. G. Lee, J. Y. Seto, T. Hirao, P. F. Bernath, and R. J. Le Roy, *J. Mol. Spectrosc.* **194,** 197–202 (1999).
45. T. Parekunnel, T. Hirao, R. J. Le Roy, and P. F. Bernath, *J. Mol. Spectrosc.* **195,** 185–191 (1999).
46. J. Y. Seto, Z. Morbi, F. Charron, S. K. Lee, P. F. Bernath, and R. J. Le Roy, *J. Chem. Phys.* **110,** 11756–11767 (1999).
47. S. A. Beaton and M. C. L. Gerry, *J. Chem. Phys.* **110,** 10715–10724 (1999).
48. Y. Liu, J. Li, D. Chen, L. Li, K. M. Jones, B. Ji, and R. J. Le Roy, *J. Chem. Phys.* **111,** 3494–3497 (1999).
49. J. L. Dunham, *Phys. Rev.* **41,** 721–731 (1932).
50. P. F. Bernath, "Spectra of Atoms and Molecules," Oxford University Press, New York, 1995.